



Use of an epiphytic lichen and a novel geostatistical approach to evaluate spatial and temporal changes in atmospheric deposition in the Athabasca Oil Sands Region, Alberta, Canada

Matthew S. Landis^{a,*}, Shanti D. Berryman^b, Emily M. White^c, Joseph R. Graney^d, Eric S. Edgerton^e, William B. Studabaker^f

^a Integrated Atmospheric Solutions, LLC, Cary, NC, USA

^b Integral Ecology Group, Duncan, BC, Canada

^c Maed Consulting, Pittsboro, NC, USA

^d Geological Sciences and Environmental Studies, Binghamton University, Binghamton, NY, USA

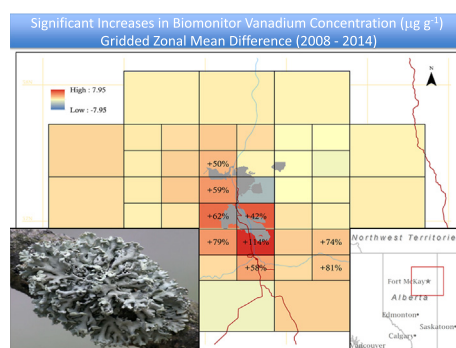
^e Atmospheric Research & Analysis, Inc., Cary, NC, USA

^f Tobacco Road Collaborative LLC, Raleigh, NC, USA

HIGHLIGHTS

- *H. physodes* is an effective indicator of gas and particulate atmospheric deposition.
- Geostatistical models were developed/evaluated to elucidate atmospheric deposition.
- Cokriging with production influence variables provided the lowest validation errors.
- Highest lichen concentrations were observed near surface oil sand production sites.
- Significant temporal and spatial deposition trends were observed between 2004 and 2017.

GRAPHICAL ABSTRACT



ARTICLE INFO

Article history:

Received 8 March 2019

Received in revised form 27 June 2019

Accepted 1 July 2019

Available online 16 July 2019

Keywords:

Lichen biomonitoring

Cokriging

Hypogymnia physodes

Atmospheric deposition

Time series analysis

Wood Buffalo Environmental Association

ABSTRACT

Temporal and spatial atmospheric deposition trends of elements to the boreal forest surrounding bitumen production operations in the Athabasca Oil Sands Region (AOSR), Alberta, Canada were investigated as part of a long-term lichen bioindicator study. The study focused on eight elements (sulfur, nitrogen, aluminum, calcium, iron, nickel, strontium, vanadium) that were previously identified as tracers for the major oil sand production sources. Samples of the in situ epiphytic lichen *Hypogymnia physodes* were collected in 2002, 2004, 2008, 2011, 2014, and 2017 within a ~150 km radius from the center of surface oil sand production operations in the AOSR. Site-specific time series analysis conducted at eight jack pine upland sites that were repeatedly sampled generally showed significant trends of increasing lichen concentrations for fugitive dust linked elements, particularly at near-field (<25 km from a major oil sands production operation) sample locations. Multiple regional scale geostatistical models were developed and evaluated to characterize broad-scale changes in atmospheric deposition based on changes in *H. physodes* elemental concentrations between 2008 and 2014. Empirical Bayesian kriging and cokriging lichen element concentrations with oil sands mining, bitumen upgrading, coke materials handling, and limestone quarry/crushing influence variables produced spatial interpolation estimates with the

* Corresponding author.

E-mail address: mlandis@atmospheric-solutions.com (M.S. Landis).

lowest validation errors. Gridded zonal mean lichen element concentrations were calculated for the two comprehensive sampling years (2008, 2014) and evaluated for spatial and temporal change. Lichen sulfur concentrations significantly increased in every grid cell within the domain with the largest increases (44–88%) in the central valley in close proximity to the major surface oil sand production operations, while a minor nitrogen concentration decrease (–20%) in a single grid cell was observed. The areal extent of fugitive dust element deposition generally increased with significantly higher deposition to lichens restricted to the outer grids of the enhanced deposition field, reflecting new and expanding surface mining activity.

© 2019 The Authors. Published by Elsevier B.V. This is an open access article under the CC BY-NC-ND license (<http://creativecommons.org/licenses/by-nc-nd/4.0/>).

1. Introduction

Anthropogenic emission of air pollutants and their potential impacts on the surrounding boreal ecosystems are a key concern in the Athabasca Oil Sands Region (AOSR) of northeastern Alberta, Canada (Percy and Krupa, 2012). As the third largest oil reserve in the world, the AOSR contains petroleum reserves estimated at 165 billion barrels (Alberta Energy Regulator, 2018). The region has undergone substantial development over the past two decades (Alberta Energy Regulator, 2018) that is projected to continue. Bitumen production levels have increased from 0.6 million barrels per day (bpd) in 2000 to 2.8 million bpd in 2017. Therefore, there is a need to understand the short- and long-term response of boreal ecosystems to atmospheric deposition of stack and tailpipe emissions as well as fugitive dust originating from oil sands development and reclamation activities.

The use of lichens, particularly epiphytic (tree-dwelling) lichens, as bioindicators of air quality is well established in the literature (Garty, 2001; Jeran et al., 2002; Nimis et al., 2002). Lichens are plants that lack a vascular system and roots, and therefore obtain their nutrients from the atmosphere, while also accumulating atmospheric contaminants. Unlike vascular plants, lichens lack a cuticle or specialized guard cells to control the exchange of water, nutrients, gases, and contaminants with the external environment. Consequently, lichens are excellent bioindicators for atmospheric deposition, incorporating both inorganic and organic air pollutants by wet and dry deposition, often accumulating these elements at levels that far exceed metabolic requirements (Garty, 2001; Nimis et al., 2002). Lichen biomonitors are particularly useful in locations such as the AOSR where they are ubiquitous, and where the active air-quality monitoring is spatially restricted due to limited road access and electrical power outside of industrialized areas (Foster et al., 2019).

Lichens have been used in the AOSR as biomonitors of air quality and atmospheric deposition in boreal ecosystems since the 1970s (Douglas and Skorepa, 1976; Wylie, 1978; Addison and Puckett, 1980; Addison, 1984; Dobbs, 1985; Pauls et al., 1996; AMEC, 2000; Berryman et al., 2004; Brenner, 2005; CE Jones, 2006). In 2004 the Wood Buffalo Environmental Association (WBEA) Terrestrial Environmental Effects Monitoring (TEEM) program established lichen biomonitors as a key component of their Forest Health Monitoring (FHM) program to complement instrument-based air quality measurements and to provide spatially resolved patterns of atmospheric deposition (Berryman et al., 2010; Edgerton et al., 2012; Graney et al., 2012; Landis et al., 2012; Graney et al., 2017; Studabaker et al., 2017; Graney et al., 2019; Landis et al., 2019a; Foster et al., 2019).

Source apportionment studies using the epiphytic lichen *Hypogymnia physodes* (L.) Nyl. as a bioindicator for atmospheric deposition have identified the main contributing sources at the local and regional scales by linking spatially-explicit elemental concentration enrichment in lichen tissue to specific contributing emissions sources in the AOSR. Results from these studies indicate that atmospheric deposition is driven by emissions from oil sands production activities (upgrader stack emissions, fugitive dust from oil sand mining, haul roads, petroleum coke materials handling, tailing ponds), mobile sources, and natural and anthropogenic biomass combustion (Landis et al., 2012; Graney et al., 2017; Graney et al., 2019; Landis et al.,

2019a). Stack emissions and mobile sources are the primary source of nitrogen deposition. Fugitive dust from oil sand production activities contributing to atmospheric deposition typically occurs within 20–30 km of the source (Edgerton et al., 2012; Graney et al., 2012; Landis et al., 2012; Graney et al., 2019; Landis et al., 2019a). Polycyclic aromatic hydrocarbons (PAH), polycyclic aromatic compounds (PAC), and lead isotopes in *H. physodes* have been used to further characterize sources contributing to atmospheric deposition in the region (Graney et al., 2017; Studabaker et al., 2017; Graney et al., 2019; Landis et al., 2019a). PAH and PAC deposition is primarily from petroleum coke and raw oil sand fugitive dust, with 90% of the PAHs and PACs being deposited within 25 km of the closest oil sand production facility (Landis et al., 2019a). Previous work has also established that fugitive dust and emissions from wildfires are important drivers of elemental enrichment in lichen and atmospheric deposition across the region.

To date, there has been no attempt to use lichen data to assess changes in atmospheric deposition patterns over time, either at the site level or spatially across the AOSR. The intent of this study is to describe spatial and temporal changes of atmospheric deposition by integrating epiphytic lichen chemical data from the WBEA-TEEM program from eight surveys over the past 16 years (2002–2017), including data from specific research studies (Berryman et al., 2004; Berryman et al., 2010; Edgerton et al., 2012; Graney et al., 2012; Landis et al., 2012; Studabaker et al., 2012; Graney et al., 2017; Landis et al., 2019a) and from the WBEA-TEEM monitoring program (CE Jones, 2006; Clair and Percy, 2015; Appendix Table A.1). Although some of these studies have included multiple lichen species, *H. physodes* was selected for this work because it has been the most consistently collected species within WBEA-TEEM lichen studies, has demonstrated high air pollution tolerance (Pfeiffer and Barclay-Estrup, 1992; Rhoades, 1999), and was identified as the optimum species for monitoring air quality of PAHs and trace elements in the AOSR (Graney et al., 2017).

This paper presents results from an integrated 2004–2017 lichen study designed to assess if significant spatial and/or temporal changes in atmospheric deposition resulted from increased oil sand development and bitumen production in the AOSR. The study utilizes two approaches to assess changes in atmospheric deposition. The first approach assesses site-specific temporal changes in lichen elemental content at eight WBEA-TEEM FHM sites common to the lichen sampling efforts between 2004 and 2017 (sampling events in 2004, 2008, 2011, 2014 and 2017). These FHM sites were consistently sampled during the 14-year period, and site-specific time-series analyses were conducted to evaluate changes in elemental concentration. The scope of this time-series analysis is limited because there were fewer sites that were commonly sampled over the 14-year period, in part, because some of the permanent monitoring locations were lost due to industrial development and wildfire (Foster et al., 2019). The second approach was to assess temporal changes in the spatial patterns of inorganic deposition at a broader regional scale between 2008 and 2014. A grid-based geospatial modeling and interpolation mapping approach was developed and evaluated for this analysis, as many lichen sample locations are unique for each survey. Other years of lichen data were not included in the grid-based mapping assessment because they did not have adequate spatial resolution to support the analysis. These two combined approaches provide an integrated examination of changes in temporal

patterns of deposition spanning a 14-year period where substantial development occurred in the AOSR.

Both approaches to evaluate trends focused on eight elements previously identified (Landis et al., 2012; Landis et al., 2017; Landis et al., 2019a; Landis et al., 2019b) as tracer species for the main sources contributing to elemental enrichment in *H. physodes*: sulfur, nitrogen, aluminum (Al), calcium (Ca), iron (Fe), nickel (Ni), strontium (Sr), and vanadium (V). Sulfur emissions are associated with bitumen upgrader stacks and fugitive dust from oil sands mining operations, and are a focus of the WBEA-TEEM program due to concerns of potential for forest soil acidification, particularly in the upland jack pine (*Pinus banksiana* Lamb.) forest ecosystems (Foster et al., 2019). Nitrogen species are emitted from upgrader stacks, mobile sources (e.g., diesel mine fleets and light duty motor vehicles), and biomass combustion. V and Ni are the petrogenic elements primarily associated with bitumen sources, such as upgrader stack emissions and fugitive dust from raw oil sands and petroleum coke. Al and Fe are marker crustal elements contained in the sand and clay soil matrix in the AOSR and are associated with fugitive dust emissions from haul roads, oil sands tailings ponds, and oil sand mining activities. Ca and Sr are signature elements for the fugitive dust from limestone quarry and crushing operations, as well as from oil sands mining haul roads constructed from limestone aggregates. PAHs and PACs were only recently (2014) integrated into the WBEA-TEEM lichen biomonitoring program (Landis et al., 2019a); therefore, we could not include these classes of compounds in this work.

2. Methods

2.1. WBEA-TEEM lichen sampling campaigns

Lichen samples were collected under the WBEA-TEEM program within an approximate 150 km radius from the center of AOSR surface oil sand production operations using three sampling approaches (i) the 2002 study utilized north-south and east-west transects centered between the Suncor and Syncrude upgrader stacks (Appendix Fig. B.1; Berryman et al., 2004), (ii) the 2004/2011/2017 campaigns were conducted at WBEA-TEEM FHM sites as part of the standard monitoring program (CE Jones, 2006; Clair and Percy, 2015), and (iii) the 2008 and 2014 studies utilized a scaled (nested) grid approach (Fig. 1; Berryman et al., 2010; Edgerton et al., 2012; Landis et al., 2019a). The approach in the 2002, 2008, and 2014 studies was to collect samples from a higher density of sites closest to the major surface mining and processing operations where steep deposition gradients were expected and to decrease sampling density further away from the surface oil sands production areas. Due to the lack of surface roads, helicopter access was the method of transportation to and from the remote sampling sites.

H. physodes data from studies in the AOSR prior to 2002 and from studies with limited sample numbers or samples collected over a very restricted geographic area were excluded from this study because the site locations were not similar across multiple years of study, or because

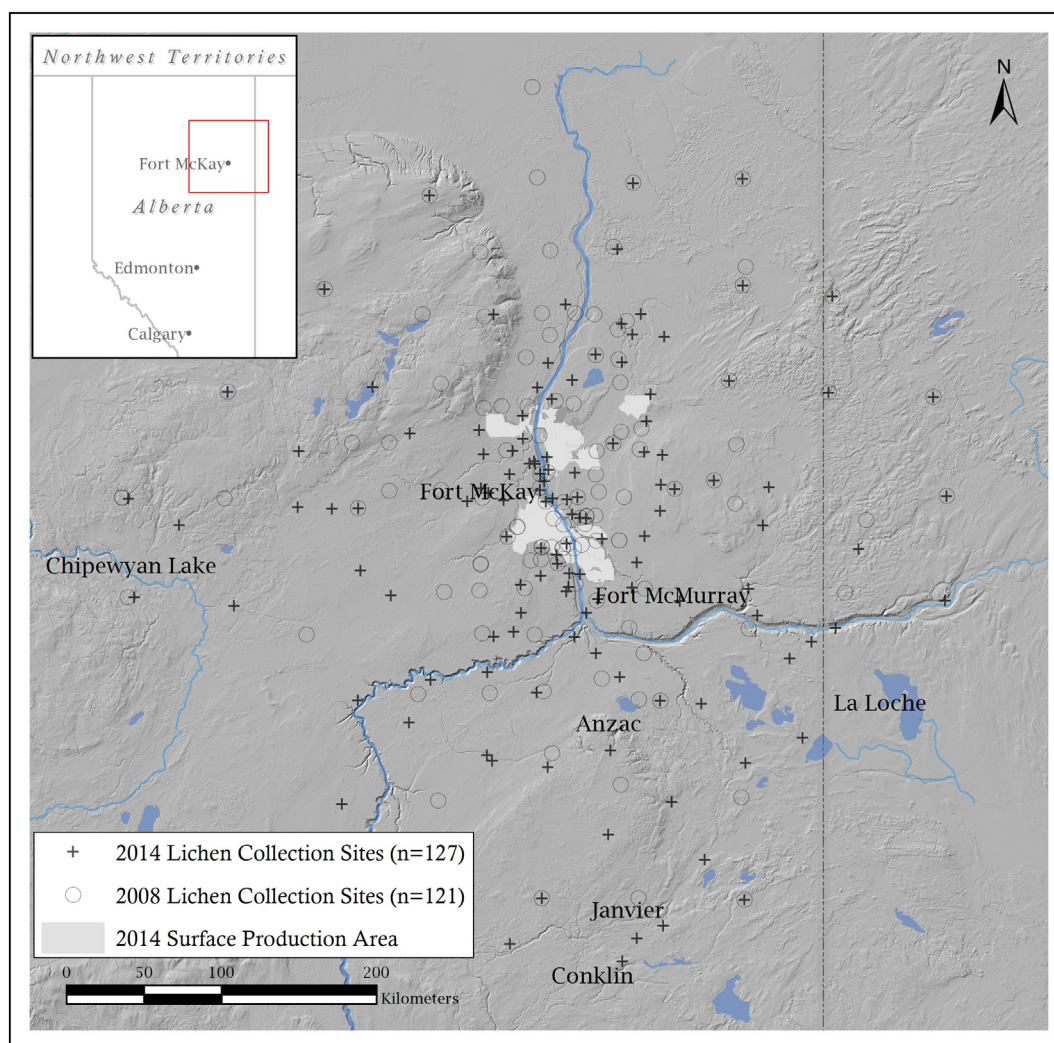


Fig. 1. Map depicting the location of the 2008 and 2014 lichen collection sites selected for multi-element analysis and the areal footprint of the 2014 oil sand production surface disturbance area. Note: Topography range is from 250 to 800 m ASL within the study domain.

the data were not directly comparable due to differences in extraction or analytical methodologies (Appendix Table A.2). All data derived from analyses of lichen species samples other than *H. physodes* were also excluded.

2.2. Collection of lichen samples

Over the years, different WBEA-TEEM program investigators participated in the collection of composite interior stand samples of *H. physodes* in the AOSR. While some minor aspects of the collection procedures may have varied, the following steps remained consistent over the years (i) lichens were collected from the branches of a minimum of 10 standing jack pine or black spruce (*Picea mariana* [Mill.] BSP) trees typically within a 25 m radius at approximately 1.5 m off the ground, (ii) sites consisted of mature stands of uniform interior trees, (iii) field personnel wearing powder-free vinyl gloves removed lichens from each tree such that the lichens collected were representative of the overall lichen community (e.g., specimen size distribution) until several grams of lichen mass were collected, and (iv) lichen individuals from all of the trees at each sampling location were composited into a sample(s) representative of the lichen population where they were collected including the range of size and presumed age of lichens at the site. Entire lichen individuals were collected for the composite sample, including the vegetative and reproductive tissues. In all cases the *H. physodes* were cleaned by removing foreign materials (bark and other lichen species) and transferred into a clean sample container, yielding several grams of mass required for all analyses and lab replicates. Cleaned samples were ground in a ball mill to homogenize the material and stored frozen ($-30\text{ }^{\circ}\text{C}$) prior to being shipped to the analytical labs for extraction and analysis.

2.3. Lichen sample extraction and analysis

Detailed methodologies and performance characteristics for the extraction and determination of total sulfur (TS), total nitrogen (TN) and element concentrations in *H. physodes* used in this study have previously been described by their respective study teams (Berryman et al., 2004; CE Jones, 2006; Berryman et al., 2010; Edgerton et al., 2012; Landis et al., 2019a) and are summarized in Appendix Table A.1. Briefly, TS concentrations were determined using dry combustion and infrared detection, TN concentrations were determined using either dry combustion and thermal conductivity or Kjeldahl wet extraction followed by colorimetric analysis, and inorganic elements were determined using either inductively coupled plasma atomic emission spectroscopy (ICP-AES) or inductively coupled plasma mass spectrometry (ICP-MS).

In most cases, the lichen data are directly comparable over the discrete sample collections, with many of the same laboratories performing the extraction and analysis using consistent protocols. The two exceptions are (i) the inorganic element concentration data from the 2002 and 2004 collection campaigns which utilized a nitric acid “partial” extraction procedure (Berryman et al., 2004; CE Jones, 2006) that likely extracts metals from the exterior and interior of lichen thalli except for metals such as Al that are bound within crystal lattices of silicate minerals (Tessier et al., 1979; White and Gubala, 1990) that are major components of fugitive dust, and (ii) the total nitrogen concentration data from the 2004 and 2008 collection campaigns which utilized dry combustion which has been shown to report significantly higher (1–6%) results versus the Kjeldahl wet extraction method for some vegetative materials (Oxenham et al., 1983; Sweeney and Rexroad, 1987; Hansen, 1989). A “total” extraction procedure was utilized on trace element samples from campaigns after 2004 (2008, 2011, 2014, 2017) which involved a multistep microwave assisted hydrogen peroxide, nitric acid, hydrofluoric acid extraction (Edgerton et al., 2012). Archived *H. physodes* samples from the 2002 study ($n = 15$) were ground, extracted using the Edgerton et al. (2012) “total” method, analyzed using ICP-MS, and compared to the original “partial”

extract ICP-AES results. For the elements evaluated here, concentrations derived from the two methods were well correlated ($p < 0.0001$). Al, Ca, Fe, Ni, and Sr had coefficients of determination (r^2) > 0.95 , and V had an $r^2 = 0.84$ (Appendix Table A.3). Therefore, the 2002 and 2004 inorganic element results were adjusted to account for their reduced sample extraction efficiencies. The magnitude of the adjustments ranged from 4% for Fe to 89% for Al (Appendix Table A.3). Archived *H. physodes* samples from the 2017 study ($n = 13$) were ground and analyzed using the dry combustion method by the British Columbia Ministry of the Environment laboratory (Victoria, BC), and the Kjeldahl wet extraction method by Pacific Soil Analysis, Inc. (Richmond, BC). The TN concentrations derived from the two methods were well correlated ($p < 0.0001$), with an $r^2 = 0.97$ (Appendix Table A.3). Therefore, the 2011, 2014, and 2017 *H. physodes* total nitrogen results were adjusted up by 8% to be equivalent to the dry combustion method.

2.4. Statistical analysis

2.4.1. Variance component analysis

The variation in elemental content in *H. physodes* samples is a function of laboratory precision (variance between laboratory replicates), field sampling precision (intra-site variance between replicate samples collected from the same site), and inter-site variation between sites (related to factors such as habitat, climate, and atmospheric deposition). Intra-site variance exists due to differences in the various lichen individuals collected at each site. This includes differences in lichen size, age, and exposure to deposition, as well as metabolic factors that may affect individual lichen uptake and accumulation of elements. The lichen sampling method was designed to minimize these intra-site variations as much as possible by collecting samples across the size and age of the entire lichen population within a given site, and by restricting sampling to interior mature stands with more uniform deposition. The component analysis assesses the magnitude of variance associated with one or more random-effects variables, in this case: site represents the inter-site variability based on field sampling from different sites; field replicates represent the intra-site variability based on lichen field replicates collected from the same site; and laboratory replicates represent the variation based on replicates of the same lichen sample re-analyzed in the laboratory. The proportion of variance for each component was calculated for four datasets used in the time-series analysis and at the site-level (2008, 2011, 2014, 2017) and focused on the key elements for this study (TS, TN, Al, Ca, Fe, Ni, Sr, V). The variance component table is reported which shows the proportion of variance attributable to these random effects. The Restricted Maximum Likelihood (REML) method was used for this analysis (Speed, 1979; See Appendix C).

Briefly, the REML method finds a set of values, the maximum likelihood estimates, at which the log-likelihood function attains its local maximum (Corbeil and Searle, 1976; Searle et al., 1992). The estimators are the variance components, and the residual variance. The maximum likelihood estimates are obtained by an iterative procedure that uses both the Newton-Raphson method and the Fisher scoring method (Jennrich and Sampson, 1976). REML variance components were derived from R (R Core Team, 2015) using the ‘lmer’ and ‘VarCorr’ commands in the lme4 package (Bates et al., 2015).

REML analysis for TS in 2011 resulted in a failed convergence of a solution (see Hartley and Rao, 1967) because the algorithms did not converge in the calculation. For this case, Analysis of Variance (AOV) analysis (see Appendix C) was used to verify the REML variance components estimates. In the traditional AOV approach, variance components are derived from sums of squares and mean squares for all effects (sites, field replicates, laboratory replicates), following the general linear model approach (Henderson, 1953; Searle, 1994). A system of linear equations is established by equating the calculated mean squares of the random effects to their expected mean squares. The variables in the equations are the variance components and the residual variance. The solution constitutes a set of estimates for the variance components.

2.4.2. Time series analysis

As part of the WBEA-TEEM monitoring program, *H. physodes* samples were collected from the FHM jack pine sites approximately every three years from 2004 to 2017 (Appendix Table A.1). Eight sites were consistently sampled for a minimum of four of the five sampling campaigns and are located at varying distances and cardinal directions from the main surface mining and bitumen upgrading operations in the AOSR (Fig. 2) representing different anticipated atmospheric deposition regimes. Time-series analysis was conducted for these eight sites to evaluate temporal changes in target elemental concentration in lichen. Data processing and time series analyses were performed using SAS software v.9.4 (SAS Institute, Cary, NC). The SAS REG and CORR procedures were used for least square general linear model regressions, and non-parametric Kendall Tau rank correlation analysis (Kendall, 1938), respectively. A level of significance of $\alpha = 0.05$ was used for the time series analysis.

2.5. Spatial interpolation and gridding

Spatial interpolation of the eight target elemental concentrations (TN, TS, Al, Ca, Ni, V, Fe, Sr) in *H. physodes* was used to elucidate spatial atmospheric deposition patterns and evaluate temporal change in the AOSR. Since the lichen sample collection was point-wise and the same locations were not all resampled during the two large sampling campaigns (2008 and 2014; Fig. 1), lichen concentration data was interpolated across the entire spatial domain and gridded mean concentrations were calculated using ESRI (Redlands, CA) ArcGIS software v.10.6.1. Both non-geostatistical and geostatistical (inverse distance weighting, ordinary kriging, ordinary cokriging, empirical

Bayesian kriging) models were evaluated (Appendix Tables A.4–A.11) through an iterative process that involved an assessment of (i) theoretical applicability, (ii) computing power requirements, (iii) cross validation error parameters, and (iv) validation fit. Once the optimal interpolation model surface was selected, the resulting prediction surface was averaged within an established regional fishnet nested grid domain (Appendix Fig. B.2) using a zonal mean approach for each element's prediction value and associated error. The model domain and subsequent grid cells were positioned to (i) be centered on the AOSR surface oil sand production area, (ii) encompass the entire domain from both the 2008 and 2014 collection years, (iii) utilize smaller nested grid cells over existing and planned production growth area, and (iv) remove grid cells for which there were no model boundary conditions for two or more domain edges and/or no samples collected for one or both years (e.g., outer four corners of domain). The 2008 nested grid zonal mean values for each target element were subtracted from their respective 2014 cell value and the resultant net temporal change (Δ_{Element}) and an evaluation of statistical significance is presented.

2.5.1. Interpolation models and parameterizations

The objective of this analysis was to quantitatively estimate spatial deposition patterns and investigate temporal trends of elemental concentration in lichen between 2008 and 2014. Several spatial interpolation models were tested and evaluated to provide the best spatially resolved estimates for spatial patterns of atmospheric deposition suitable for this investigation. Each of the methods evaluated are discussed, including their relevant assumptions, advantages, and limitations.

Inverse distance weighting (IDW) is a deterministic model that is appropriate for initial screening of spatial data. The IDW model is not

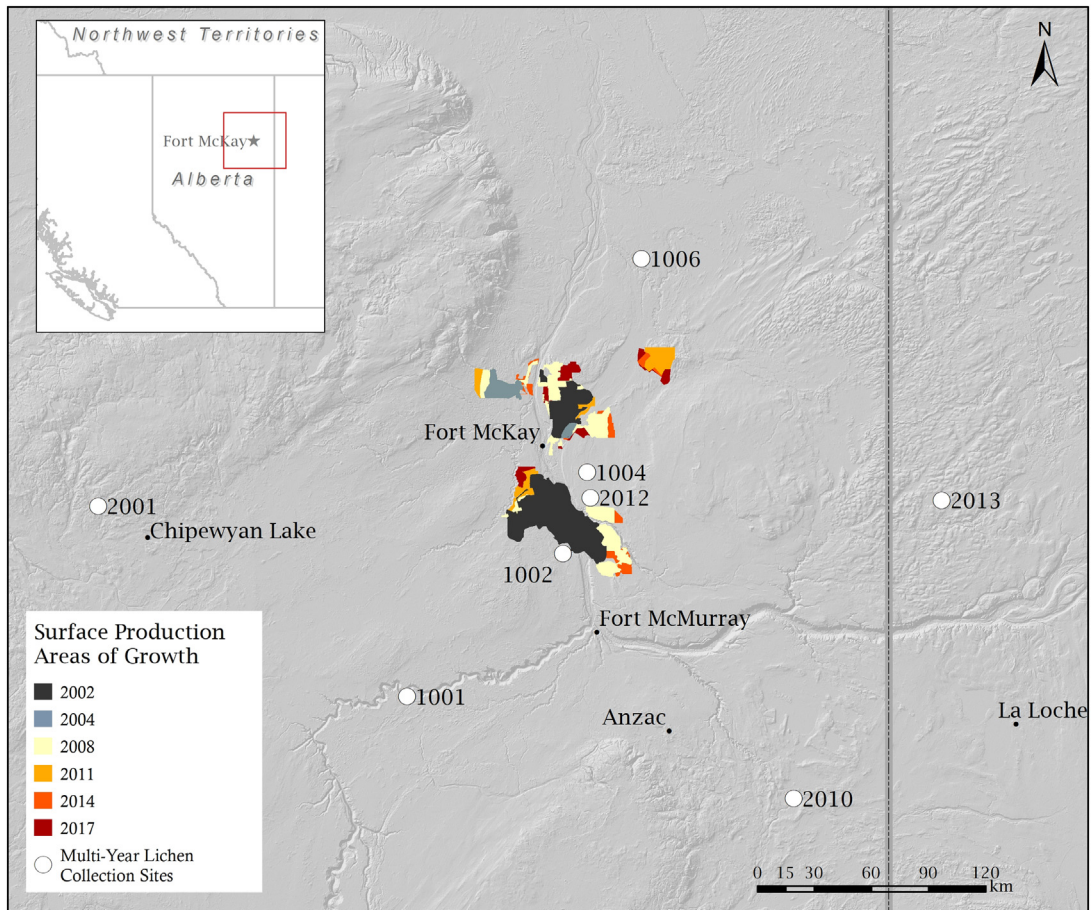


Fig. 2. Map depicting the location of the long-term forest health monitoring lichen collection sites and the expanding areal footprint of oil sand production surface disturbance area during the study period.

computing power intensive, there are no data assumptions, it requires minimal parametrization, and it provides a general shape of each interpolation surface. It is however, an exact interpolator, meaning all sample site concentrations remain fixed in the resultant interpolation surface, producing a characteristic “bullseye” effect particularly when large and irregular concentration gradients are present. Because the IDW model does not provide an estimate of prediction error, it was used as an initial data screening tool to visualize the interpolated deposition surfaces and as a check when evaluating geostatistical methods.

We ran and evaluated a series of kriging spatial interpolation methods, where “Kriging” is a generic name for a family of generalized least-squares regression algorithms (Krige, 1951) used for geostatistical modeling when spatially resolved data exhibits a spatial dependency (Li and Heap, 2008). Kriging is an appropriate tool when used on data that demonstrates a correlation between samples that varies by distance, and this correlation decreases as the distance increases. The spatial dependency is explored and expressed in Kriging using a semi-variogram. A strong spatial dependence is numerically easy to fit, while a weak spatial dependency leads to difficulty in fitting a variogram and weak cross-validation/validation prediction error statistics. Both classical statistical and geostatistical methods perform best with normally distributed data, and this is especially important in kriging. Simple kriging (SK) assumes a constant mean and distribution throughout the sample domain, ordinary kriging recalculates local means across the modeled area. Cokriging can be applied to any base model and gives the user the ability to use a secondary variable to assist in modeling spatial variance (e.g., elevation can be used as a secondary auxiliary variable to predict ambient temperature at unmeasured locations), and a cross variogram between the two data sets is defined.

Raw Variograms were generated in ArcGIS for each data set's semivariance, γ ; versus distance between all data point pairs, h , for all data points of lichen concentration Z_x as expressed in Eq. (1).

$$\gamma(h) = \frac{1}{2} [(Z_{x+h} - Z_x)^2] \quad (1)$$

An initial Theoretical Variogram - a fit to the Experimental Variogram (binned average semivariance) and the curve to which the resultant spatial model - is then created. The final theoretical variogram fit was chosen through iterative cross validation. Gaussian or spherical (stationary, bounded) variogram fits were chosen such that variograms always reached a sill or maximum variance, as linear or exponential (unbounded) fits would not describe lichen elemental concentrations with distance (Edgerton et al., 2012; Landis et al., 2019a). While the atmosphere theoretically maintains no barriers and a nugget may be assumed to be zero, the model was allowed to calculate a nugget (discontinuity in γ when distance $h = 0$) because of variation in elemental content in the lichen and local scale variability. A measurement error of 100% was applied to all model runs. As a result, the kriging algorithm is both an inexact interpolator and accounts for sample/analytical error as well as any intra-site variance.

All model run parameters are presented in Appendix Tables A.4–A.11. Measures of unbiasedness, minimal variance, and the validity of the uncertainty were evaluated using (i) ArcGIS single point cross-validation iterative process and (ii) user employed validation, in which a randomly selected subset consisting of 10% of the overall data points was identified and removed, the model rerun, and the removed data set points estimated. Models were evaluated based on the best unbiased linear approach (centered on measurements) such that the mean of the prediction error estimation would be as close to zero as possible, and the variance was minimized as evaluated through the mean square estimation error as described by Lantuejoul (2002). The precision of each models' interpolation estimates to measured samples were evaluated through the root-mean-square prediction error (Appendix Tables A.4–A.11).

All predicted surface maps for the elements of interest, including the exploratory IDW surfaces (Appendix Fig. B.3a–p), indicate significant gradients and large-scale variation in lichen elemental concentrations, decreasing in concentration with increasing distance from surface oil sand mining and production facilities (Graney et al., 2012; Landis et al., 2012; Landis et al., 2019a), indicative of a mean that is not constant within our sampling domain, which violates the basic kriging model data stationary assumption (that the mean and semivariance depends only on the distance between the data points and not the absolute location of data collection). There are several ways to deal with a variable mean or “trend”: (i) remove a 1st, 2nd or 3rd order polynomial trend and apply ordinary kriging to the resultant data, (ii) use empirical Bayesian kriging (EBK; Krivoruchko, 2012; Javari, 2017), or (iii) use cokriging. Based on objective evaluations of spatial prediction error discussed in Section 3.3, cokriging and EBK were chosen as the best performing spatial interpolation methods.

2.5.2. Lichen concentration data transformation

All eight target element concentrations, from both 2008 (Appendix Table 12) and 2014 (Appendix Table 13) collections, exhibited distributions that were significantly different from normal. Log transformation improved skewness and kurtosis (Sheskin, 2000; Appendix Table A.14). Interpolation through kriging is ideal when the data input distribution is Gaussian, so all data were log transformed prior to kriging model application, and ArcGIS inverse log transform (anti-logs) the data prior to final output generation.

2.5.3. Lichen concentration data trend removal

Trend removal evaluates an overriding physical process that affects all measurements in a deterministic manner. In the AOSR, the trend is driven by known anthropogenic emission source location, topography, and dominant local/synoptic wind patterns (Davies, 2012; Landis et al., 2019a). Removing the surface trends from the data and using kriging on the detrended, residual data may account for the underlying known physical factors. The overall “signal” must be removed to evaluate the finer structure of the “noise”. While a simple polynomial trend removal was advantageous (Appendix Tables A.4–A.11; ordinary kriging, 2nd or 3rd order polynomial trend removal) in reducing average prediction errors in many instances, this was not the case for all elements, making it apparent that a higher order approach to trend analysis was appropriate. To achieve this, spatially and temporally resolved local emission information (Foster et al., 2019) was used to estimate the underlying atmospheric deposition field trends and was utilized as cokriging auxiliary variables. From previous work, we have shown an exponential relationship between distance to source and all elements presented (Landis et al., 2019a). Four heterotopic data auxiliary surfaces representing the four major oil sand production emission source influences (oil sand mining, bitumen upgrading, petroleum coke production and storage, limestone quarrying and crushing) were developed and evaluated for significance in reducing the dominant regional atmospheric deposition field for each collection year. All lichen sampling sites (Fig. 1) combined with a set of 2688 (56×48) equally spaced grid points (Appendix Fig. B.4) were used to create an array of points across the AOSR domain and an annual production influence (PI) surface, a dimensionless measure of the effect of each local surface oil sand production emission source type on each point was calculated using Eq. (2).

$$PI(E, S) = \sum_{i=1}^n f(d \times pr) \quad (2)$$

where PI for each target element (E) and each emission source type (S) is the sum of all the individual emission sources (Landis et al., 2019a) influence on each grid point. The distance function $f(d)$ is an annual analyte specific weight that varies by the distance (d) of each emission source location to each grid point using the empirically derived

exponential decay function presented in Appendix Fig. B.5 (2008) and Appendix Fig. B.6 (2014), and the relative influence of each emission source was weighted by its annual production rate (*pr*). *PIs* were calculated for 2008 and 2014 oil sand mines, bitumen upgrader stacks, petroleum coke production and storage, and limestone quarry and crushing operations. The significance of each *PI(E,S)* surface in detrending the target element specific regional surface layer was tested using the SAS v.9.4 GLM procedure for multiple regressions analysis comparing the *PI(E,S)* value to the *H. physodes* concentration at each sampling site and the results are summarized in Appendix Table A.15 (2008) and Appendix Table A.16 (2014). Only those *PI(E,S)* surfaces found to have significant ($\alpha = 0.05$) Type III partial sum of squares *P* values were utilized in the cokriging model (Searle, 1987), with the exception of 2014 TN where $\alpha = 0.10$ was utilized to allow a single *PI(E,S)* surface to be utilized (Appendix Table A.16).

EBK is the final method employed to address the underlying deposition trend as reflected by elemental concentrations in lichen. The EBK model is advantageous in that the intrinsic random function corrects for trends, and unlike kriging models (i) does not assume an overall mean, (ii) requires minimal user input because it automatically produces the semivariogram based on a bootstrap-like subset simulation, and (iii) generates accurate prediction errors. The disadvantages include significant computational processing time and inability to account for major trends. A K-Bessel Detrended semivariogram was chosen for all target element runs. Validation was completed for all valid trend-removed methods, ordinary kriging with polynomial trend removal, cokriging, and EBK models and is presented in Appendix Tables A.4–A.11.

2.5.4. Evaluating spatially resolved changes in atmospheric deposition

Fishnet zonal means of *H. physodes* elemental concentrations were utilized to calculate regional gridded atmospheric deposition estimates allowing for the quantification of local and regional scale temporal changes in the AOSR between the 2008 and 2014 collection years. Grids were built using the fishnet algorithm within ArcGIS, and a consecutive alphabetical and numerical naming system was created (Appendix Fig. B.2). Outer, regionally reflective grids (A2–6, B1, B8, D1, D8, F1, F8, H2–6) are approximately 56 km × 42 km, and the central, smaller, proximal grids (B2–7, C2–7, D2–7, E2–7, F2–7, G2–7) are approximately 27 km × 21 km, with incremental changes in the grid size along the north south transect due to geographic projection characteristics. An ArcGIS ‘minus’ function was applied to each grid’s polygon average lichen concentrations to calculate a delta (Δ_{Element}) change in the concentration for each cell and target element over the 2008–2014 time period. Grid-specific mean prediction errors were also calculated and used to test for significant change between the 2008 and 2014 gridded concentrations. For each grid and target element, the concentration was considered significantly different if both collection year values \pm mean prediction errors were mutually exclusive.

3. Results and discussion

3.1. Effectiveness of *Hypogymnia physodes* as a biomonitor in the AOSR

3.1.1. Lichen sample variability - variance component analysis

The variance associated with laboratory replicates and intra-site replicates in most cases is <15% of total variance indicating that the methods employed in lichen biomonitoring in the AOSR can effectively characterize site-to-site changes in elemental concentrations of *H. physodes* at local and regional scales. The variability associated with laboratory measurements is typically related to measurement imprecision (e.g., values close to the detection limit), was always smaller than inter-site variability, and was generally the smallest source of variance due to robust laboratory methods for homogenization of ground composite lichen samples, digestion, and recovery (Table 1; Edgerton et al., 2012). Intra-site variation was always smaller than inter-site

Table 1

Study specific inter-site, intra-site, and laboratory variance components for elemental concentrations in *H. physodes* samples. (Note that there were no lab replicates for total nitrogen and total sulfur in 2017).

| Element | Variance components: proportion | | |
|----------------|---------------------------------|------------|------------|
| | Inter-site | Intra-site | Laboratory |
| 2008 | | | |
| Total Sulfur | 0.705 | 0.099 | 0.197 |
| Total Nitrogen | 0.958 | 0.032 | 0.010 |
| Aluminum | 0.961 | 0.038 | 0.002 |
| Calcium | 0.984 | 0.016 | 0.001 |
| Iron | 0.989 | 0.011 | 0.001 |
| Nickel | 0.885 | 0.105 | 0.009 |
| Strontium | 0.994 | 0.005 | 0.001 |
| Vanadium | 0.870 | 0.127 | 0.002 |
| 2011 | | | |
| Total Sulfur | 0.749 | 0.251 | <0.001 |
| Total Nitrogen | 0.931 | <0.001 | 0.069 |
| Aluminum | 0.987 | 0.008 | 0.005 |
| Calcium | 0.989 | 0.013 | 0.001 |
| Iron | 0.992 | 0.007 | 0.001 |
| Nickel | 0.989 | 0.002 | 0.010 |
| Strontium | 0.989 | 0.007 | 0.005 |
| Vanadium | 0.988 | 0.009 | 0.002 |
| 2014 | | | |
| Total sulfur | 0.948 | 0.045 | 0.007 |
| Total nitrogen | 0.927 | 0.065 | 0.008 |
| Aluminum | 0.968 | 0.031 | 0.001 |
| Calcium | 0.985 | 0.015 | <0.001 |
| Iron | 0.978 | 0.021 | 0.001 |
| Nickel | 0.962 | 0.035 | 0.003 |
| Strontium | 0.958 | 0.042 | <0.001 |
| Vanadium | 0.958 | 0.041 | <0.001 |
| 2017 | | | |
| Total sulfur | 0.866 | 0.067 | – |
| Total nitrogen | 0.997 | 0.002 | – |
| Aluminum | 0.945 | 0.053 | 0.002 |
| Calcium | 0.934 | 0.065 | 0.001 |
| Iron | 0.979 | 0.020 | 0.002 |
| Nickel | 0.919 | 0.080 | 0.001 |
| Strontium | 0.950 | 0.049 | 0.002 |
| Vanadium | 0.920 | 0.079 | 0.001 |

variability, indicating that the lichen samples were representative of their sampled lichen populations within each site (Table 1).

3.1.2. Comparison of elemental concentration in *H. physodes* to published values

Concentrations of elements in *H. physodes* in this study were compared to other values reported in the scientific literature (Appendix Table A.17). *H. physodes* is pollution-tolerant and common in the Northern Hemisphere, and consequently there is a wealth of literature on the use of this lichen species as an in situ or transplanted bioindicator of air pollution atmospheric deposition. The literature review we present for *H. physodes* is representative of studies that seek to establish both background concentrations and elevated concentrations associated with specific sources. Comparisons of elemental concentrations did not take into consideration laboratory methods or other sampling and processing methodology, and we recognize that this can introduce substantial variability among published values. Many studies only report on a small set of elements, and levels for Sr and V have rarely been published.

The AOSR *H. physodes* samples exhibited a broad range of concentrations for all elements. Samples collected from near source sites are comparable to or higher than those published in the scientific literature, including TN, TS, Al, Ca, and Fe (Appendix Table A.17). In contrast, elemental concentrations at distal sites are comparable to low or background levels reported elsewhere (Appendix Table A.17). This indicates that the regional study domain for lichen biomonitoring in the AOSR (as captured by the broader scale sampling efforts in 2008

and 2014) effectively span the elemental concentration gradient reported in the literature. Ni concentrations in the AOSR fall within the range of reported values for both low/background and elevated deposition sites (Appendix Table A.17). Levels of Sr in lichens sampled in the AOSR fall within range of published values, and the highest V concentrations in the AOSR in this study are much lower than those previously measured in the AOSR in the late 1970s (Addison and Puckett, 1980) prior to oil sands operators installing emission controls on upgrading stacks.

TN levels in *H. physodes* were elevated in the AOSR and are comparable to other high nitrogen deposition areas in Norway, Finland, and the United States. TS levels in *H. physodes* are comparable to other high sulfur deposition areas in Finland, Norway, and Switzerland, but in some cases published TS values are greater than those measured in the AOSR lichen samples. This suggests that the TN and TS levels in *H. physodes* are elevated in places in the AOSR, but that they have not reached an upper threshold of TN and TS accumulation. Concentrations of Al, Fe, and Ca in some lichen samples from the AOSR are much greater than any published values, where the greatest Ca levels in *H. physodes* of the AOSR are almost a factor of three higher relative to the highest published value elsewhere (Wetmore, 1987). Al, Ca, and Fe are key tracers of fugitive dust emissions in the AOSR, where lichens growing near surface development activity are subjected to high depositional fluxes. It is unknown what the thresholds of accumulation of these elements are for *H. physodes*, and if these may be met at sites with heavy fugitive dust loading in the AOSR.

3.2. Site specific deposition time series analysis (2004–2017)

Results from the WBEA-TEEM FHM site-specific time series analysis generally showed trends of increasing concentrations of elements in lichen from 2004 to 2017. Time series plots with least squares linear regression models for eight sites and the eight target elements are presented in Appendix Figs. B.7–B.14, with 63 of the 64 regression slopes presented being positive. The p values for all the FHM site regressions and non-parametric Kendall Tau rank correlation coefficients are summarized in Table 2. In general, the sites near the surface oil sand mining and upgrading operations (1002, 1004, 2012; Fig. 2) were associated with the highest overall element concentrations in lichen, the steepest rates of increase, and the most significant trends. The concentrations of elements most associated with fugitive dust from surface oil sands production operations (Landis et al., 2012; Landis et al., 2017; Landis et al., 2019a; Landis et al., 2019b) were most likely to have significantly increasing trends at near field sites 1002 (Al, Ca, Fe,

Sr, V), 1004 (Al, Ca, Fe, Sr, TS, V), and 2012 (Al, Ca, Fe, Ni, Sr, V). Whereas sites further away from the surface oil sand mining and upgrading operations (1001, 1006, 2001, 2010, 2013) were generally associated with the lowest concentrations, lowest rate of accumulation, and least number of significant trends. The more distant locations had relatively few significantly increasing trends, including sites 1001 (Fe), 1006 (Al, Fe), 2001 (Al, Fe, TN), 2010 (Al, Ni), and 2013 (Al, Fe, V). The enhancement ratios describing the changes in elemental concentrations between 2004 and 2017 for each of the sites and elements are presented in Appendix Table A.18.

To illustrate these trends, the lichen TS, TN, Al, and V concentration time series plots from one near field jack pine site (1004) and one more distant jack pine site (2001) are presented in Fig. 3. The proximal site (1004) is located ~11 km east (predominantly downwind) of surface oil sand mining, bitumen upgrading, and limestone quarrying/crushing operations, and the distal site (2001) is located ~120 km west of the nearest oil sand mining operation. TS in the AOSR is associated with both gaseous sulfur dioxide emissions from the upgrading of sour bitumen to sweet synthetic crude as well as fugitive dust from oil sand mining operations (Landis et al., 2017; Phillips-Smith et al., 2017; Landis et al., 2019b). The TS concentration at site 1004 significantly ($p = 0.04$) increased between 2004 (0.086%) and 2017 (0.159%) by an average of 0.005% per year (Fig. 3a) equating to an overall enhancement ratio of 1.9. The rate of TS increases over the last three sample collections between 2011 and 2017 at site 1004 was more significant ($p = 0.004$) and more than double (0.011% per year) the overall study period accumulation rate indicating an accelerating atmospheric deposition trend. The lichen TS concentration trend at site 2001 (Fig. 3b) did not significantly change between 2004 (0.065%) and 2017 (0.073%), which was consistent with the lack of a significant trends in TS for the more distant FHM sites (1001, 1006, 2001, 2010, 2013; Table 2; Appendix Fig. B.7).

Lichen TN concentrations in the AOSR are primarily driven by gaseous emission of nitrogen oxides and ammonia from the combustion of fossil fuels for bitumen upgrading and mobile source transportation (e.g., mine heavy hauler fleet and light duty vehicles), and wildland fires (Landis et al., 2017; Landis et al., 2018; Foster et al., 2019; Landis et al., 2019a; Landis et al., 2019b). The observed trend for lichen TN concentration was unique in that the proximal site 1004 (Fig. 3c) did not demonstrate a significant change between 2004 (0.670%) and 2017 (0.910%), however the distal site 2001 (Fig. 3d) site did indicate a significant ($p = 0.03$) increasing trend from 0.449% in 2004 to 0.677% in 2017 equating to an overall ER of 1.5. Interestingly, the TN values at all the FHM jack pine sites were noticeably higher across the entire sampling

Table 2
Summary of linear least squares regression and Kendall Tau hypothesis tests, evaluating if there was significant change in *H. physodes* elemental concentrations between 2004 and 2017.

| Element | Test | p-Values by sampling site | | | | | | | |
|----------------|-------------|---------------------------|----------------|--------------|--------------|--------------|--------------|----------------|----------------|
| | | 1001 | 1002 | 1004 | 1006 | 2001 | 2010 | 2012 | 2013 |
| Aluminum | Regression | 0.053 | 0.004 | 0.002 | 0.157 | 0.027 | 0.065 | 0.009 | < 0.001 |
| | Kendall Tau | 0.174 | 0.014 | 0.014 | 0.042 | 0.042 | 0.042 | 0.050 | 0.042 |
| Calcium | Regression | 0.633 | 0.030 | 0.025 | 0.482 | 0.603 | 0.342 | 0.008 | 0.956 |
| | Kendall Tau | 0.497 | 0.142 | 0.014 | 0.497 | 0.174 | 0.497 | 0.014 | 0.497 |
| Iron | Regression | 0.022 | 0.004 | 0.002 | 0.110 | 0.004 | 0.260 | 0.028 | 0.015 |
| | Kendall Tau | 0.042 | 0.014 | 0.014 | 0.042 | 0.042 | 0.497 | 0.050 | 0.042 |
| Nickel | Regression | 0.791 | 0.017 | 0.134 | 0.551 | 0.707 | 0.259 | 0.014 | 0.195 |
| | Kendall Tau | 1.000 | 0.014 | 0.142 | 0.497 | 0.497 | 0.042 | 0.050 | 0.497 |
| Strontium | Regression | 0.125 | < 0.001 | 0.009 | 0.205 | 0.209 | 0.121 | < 0.001 | 0.242 |
| | Kendall Tau | 0.174 | 0.014 | 0.014 | 0.174 | 0.497 | 0.174 | 0.014 | 0.174 |
| Total nitrogen | Regression | 0.549 | 0.201 | 0.355 | 0.081 | 0.025 | 0.142 | 0.069 | 0.083 |
| | Kendall Tau | 0.624 | 0.207 | 0.624 | 0.174 | 0.071 | 0.142 | 0.142 | 0.174 |
| Total sulfur | Regression | 0.599 | 0.186 | 0.043 | 0.238 | 0.530 | 0.174 | 0.127 | 0.174 |
| | Kendall Tau | 0.624 | 0.372 | 0.050 | 0.174 | 0.497 | 0.327 | 0.142 | 0.497 |
| Vanadium | Regression | 0.108 | 0.004 | 0.011 | 0.240 | 0.244 | 0.182 | 0.052 | 0.025 |
| | Kendall Tau | 0.174 | 0.014 | 0.050 | 0.174 | 0.174 | 0.174 | 0.050 | 0.042 |

Bold text denotes significance at $\alpha = 0.05$.

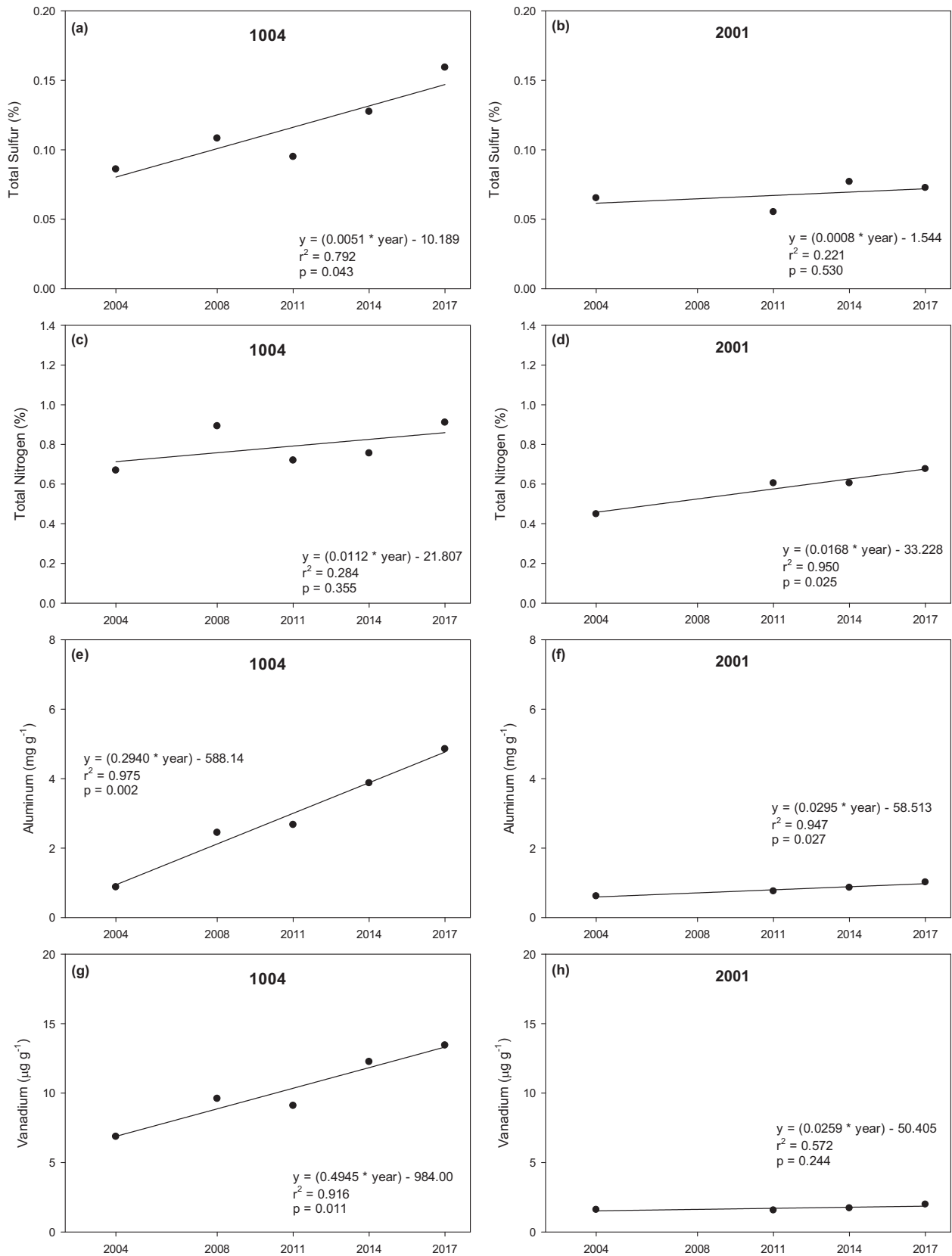


Fig. 3. Time series plots of elemental concentration in *H. physodes* (2004–2017) at sites 1004 and 2001.

domain in the 2008 collection (Appendix Fig. B.8). However, even if the 2008 value at site 1004 was removed the linear trend would still not be significant ($p = 0.13$).

Al is a crustal element primarily associated with fugitive dust sources in both ambient fine and coarse fraction particulate matter (Landis et al., 2017; Phillips-Smith et al., 2017; Landis et al., 2019b)

and lichens (Landis et al., 2019a) in the AOSR. The Al concentration at proximal site 1004 significantly ($p = 0.002$) increased between 2004 (0.88 mg g^{-1}) and 2017 (4.85 mg g^{-1}) by an average of $\sim 0.3 \text{ mg g}^{-1} \text{ y}^{-1}$ (Fig. 3e) equating to an overall enhancement ratio of 5.6. The significance and observed trend in Al enhancement was similar to Sr (5.4) and Ca (5.9) at site 1004 (Table 2; Appendix Figs. B.11 and B.14), indicative of a large and continuing fugitive dust impact from near-field oil sand production and transportation sources (e.g., mine haul roads, unpaved highways). The Al concentration at distal site 2004 (Fig. 3f) also significantly ($p = 0.027$) increased between 2004 (0.62 mg g^{-1}) and 2017 (1.02 mg g^{-1}), which was consistent with similar significant trends at some of the other distal sites (Appendix Fig. B.12). The magnitude of change at the 2001 distal site was almost an order of magnitude lower ($\sim 0.03 \text{ mg g}^{-1} \text{ y}^{-1}$) than rate of change at site 1004 ($\sim 0.3 \text{ mg g}^{-1} \text{ y}^{-1}$) consistent with the observed exponential decrease in atmospheric deposition of coarse fraction particulate matter as a function of distance from the closest surface oil sand production operation (Appendix Figs. B.5 and B.6; Landis et al., 2019a).

V is a petrogenic element and is primarily associated with fugitive oil sand mine dust and upgrader stack emissions in ambient particulate matter (Landis et al., 2017; Phillips-Smith et al., 2017; Landis et al., 2019b) and in lichen (Landis et al., 2019a) in the AOSR. Lichen V concentration at proximal site 1004 significantly ($p = 0.011$) increased between 2004 ($6.86 \text{ } \mu\text{g g}^{-1}$) and 2017 ($13.44 \text{ } \mu\text{g g}^{-1}$) by an average of $\sim 0.5 \text{ } \mu\text{g g}^{-1} \text{ y}^{-1}$ (Fig. 3g) equating to an overall enhancement ratio of 2.0, consistent with the significant increases at the other two proximal sites 1002 (enhancement ratio = 2.6) and 2012 (enhancement ratio = 2.5). The lichen V concentration at the distal site 2001 (Fig. 3h) did not significantly change between 2004 ($1.60 \text{ } \mu\text{g g}^{-1}$) and 2017 ($1.99 \text{ } \mu\text{g g}^{-1}$) consistent with other distal sites 1006, 2001, and 2010 (Appendix Fig. B.9). Site 2013 was the sole distal location where a small (enhancement ratio = 1.5) but significant ($p = 0.025$) increase in lichen V concentration was observed (Appendix Fig. B.9). Site 2013 is $\sim 96 \text{ km}$ due east (predominantly downwind) of a major surface oil sands mining operation and $\sim 105 \text{ km}$ east of the closest major upgrader stack.

Results from the time-series analysis demonstrate the value of lichen biomonitoring as part of the WBEA-TEEM FHM program to track changes in deposition over time at each site. The temporal changes of elements in lichen appear generally consistent with regional patterns of atmospheric deposition (Edgerton et al., 2019), but further investigation is needed for direct comparisons of lichen and deposition data. The scope of inference for these results is restricted to jack pine uplands, and the eight sites that span the range of observed regional depositional gradients (Landis et al., 2019a). WBEA-TEEM expanded the FHM site network in 2011, including sampling of lichens, which will result in additional sites for future time-series assessments.

3.3. Spatially resolved deposition time series analysis for the AOSR (2008–2014)

Multiple regional scale geostatistical models were developed and evaluated to characterize broad-scale changes in atmospheric deposition based on changes in *H. physodes* elemental concentrations in the AOSR between 2008 and 2014, the two large region-wide lichen sampling campaigns. An iterative process of optimizing spatial modeling parameters using objective ArcGIS cross-validation and validation evaluation procedures was undertaken to produce geostatistical models with the lowest achievable interpolation errors in the AOSR. The log transformation of the lichen analytical data always produced better spatial interpolation results. Incremental decreases in interpolation error were observed when (i) 2nd or 3rd order polynomial trends were removed, (ii) the auxiliary variable of Production Influence (PI) was used in cokriging, and (iii) the EBK model was employed.

Overall, cokriging with PI variables (oil sands mining, bitumen upgrading, petroleum coke production and storage, and limestone quarrying/crushing) and EBK produced the optimum balance between

reduction in estimation error and reproduction of the screening level IDW exact interpolated surfaces. The best model was selected for each element based on objective validation criteria including cross validation, validation, estimation error, and linear regression analysis (Appendix Tables A.4–A.11). Cokriging model estimates were utilized for TS, TN, Al, Fe, Ni, and V, while EBK model estimates were utilized for Ca and Sr. Interpolation maps were generated from the geostatistical models to provide a visual representation of the regional atmospheric deposition patterns for the target elements, and gridded zonal mean concentrations were calculated for the evaluation of spatial and temporal change across the AOSR (Figs. 4–8; Appendix Figs. B.15–17). Due to substantial differences in the absolute distribution and range of elemental concentrations between the 2008 and 2014 lichen collections, isopleth solid contours of the final interpolation maps (Figs. 4–8a–b; Appendix Figs. B.15–17a–b) were color-scaled in order to present the best visual spatial representation of the deposition field and concentration gradients for each respective year. The concentration differences between the 2008 and 2014 collections can be directly compared when viewing the gridded results (Figs. 4–8c–d; Appendix Figs. B.15–17c–d), as the color scales have been normalized between the two collection years.

3.3.1. Total sulfur

The spatial pattern of TS concentrations in lichen retained its general shape, but the area of maximum concentration increased in size between 2008 (Fig. 4a) and 2014 (Fig. 4b). The observed increases in TS concentrations were significant for every grid cell within the domain (Fig. 4e; Appendix Fig. B.18a) with the most dramatic increases ranging from 44 to 88% in the central nested grid spaces (D4, E4, E5) in close proximity to the largest surface oil sand mines and bitumen upgrading operations. This likely reflects the expansion of mining operations and the resulting increases in bitumen extraction, and the amount of bitumen upgraded to synthetic crude between 2008 and 2014 (Foster et al., 2019).

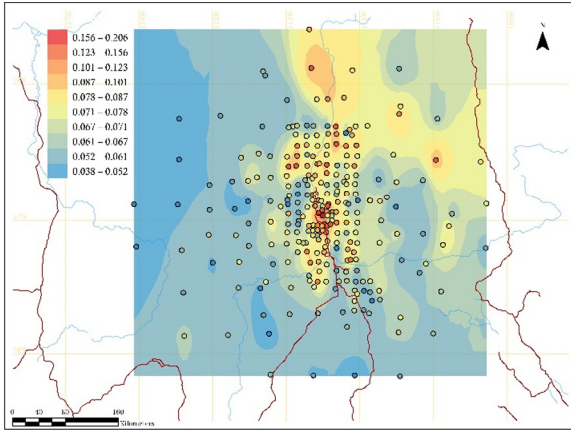
3.3.2. Total nitrogen

A general pattern of decreased TN concentrations in lichen between 2008 (Fig. 5a) and 2014 (Fig. 5b) was evident for much of the domain, although the change was only significant in a single grid (F5) south of the main surface oil sand production operations amounting to a decrease of 20% (Fig. 5e; Appendix Fig. B.18b). The dichotomy between the site-specific time series analysis suggesting generally increasing TN deposition between 2004 and 2017 and the spatially resolved gridded analysis is due solely to the higher 2008 campaign sample results (Appendix D). The 2008 TN results may be the result of regional/synoptic meteorological conditions (e.g., precipitation amount/type, temperature, winds) that modulated regional nitrogen deposition (Edgerton et al., 2019); future lichen collection data will be able to extend the spatially resolved data record and bring more clarity to the general regional trend in TN atmospheric deposition.

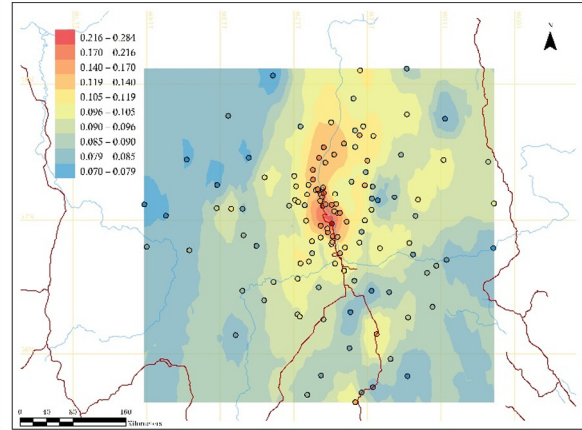
3.3.3. Aluminum and iron

As tracers for soil, haul road, and tailings fugitive dust in the AOSR (Landis et al., 2012; Landis et al., 2017), Al and Fe concentrations in lichen expanded in extent from the central surface mining operations in 2008 (Fig. 6a; Appendix Fig. B.15a) to 2014 (Fig. 6b; Appendix Fig. B.15b). A new area of elevated concentrations in the southern portion of the domain adjacent to the roadway network between Anzac and Conklin in an area containing in situ production sources was observed (Fig. 6b; Appendix Fig. B.15b) as described in Landis et al., 2019a, however the increase was not significant in the associated grids (H4, H5). Gridded areas of significant increase corresponded to (i) the central area of the modeling domain, where surface production activities increased between the two years (Fig. 6e; Appendix Fig. B.15e) resulting in zonal mean lichen concentration increases between 38–258% (Al) and 47–127% (Fe), and (ii) in the southeast portion

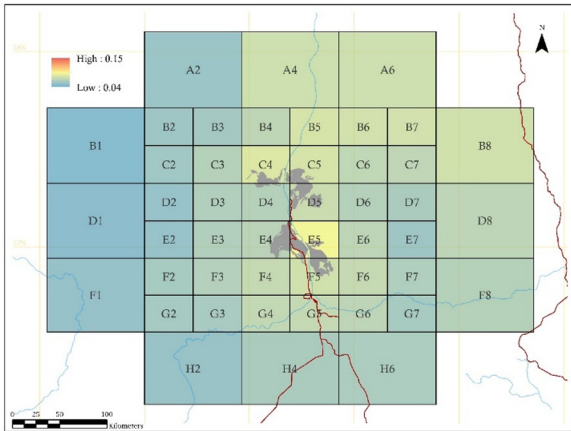
a. 2008 observed points and predicted surface



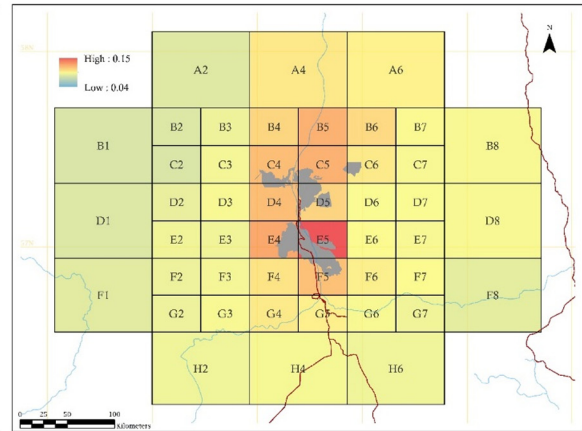
b. 2014 observed points and predicted surface



c. 2008 gridded zonal mean concentrations



d. 2014 gridded zonal mean concentrations



e. ΔT_S (2008 to 2014) gridded zonal mean concentrations with significant percent increase in all grids

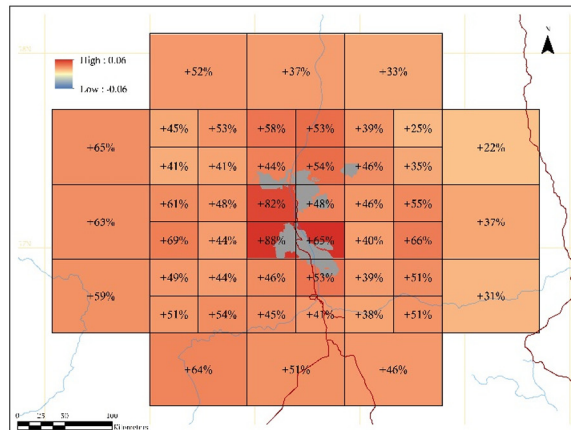


Fig. 4. Spatial and temporal analysis of total sulfur (%) 2008–2014 using cokriging.

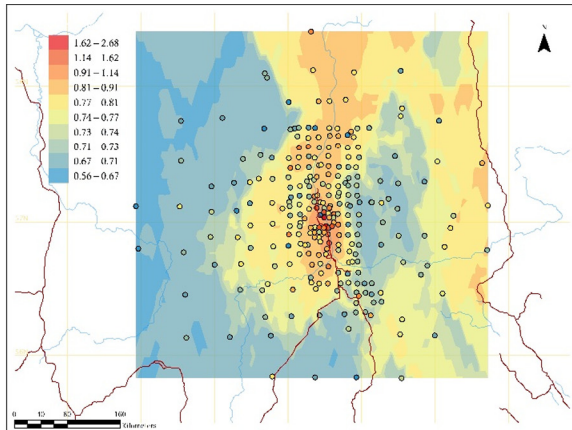
of the domain in grids F7 and G7 resulting in zonal mean lichen concentration increases between 64–67% (Al; Appendix Fig. B.18c) and 65–73% (Fe; Appendix Fig. B.18d).

3.3.4. Nickel and vanadium

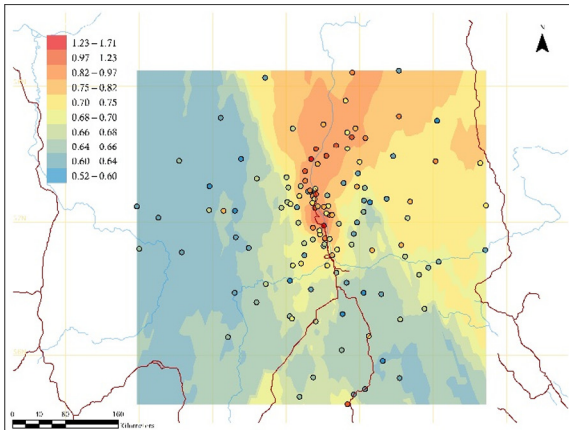
Ni and V are petrogenic elements that are common tracer species for surface oil sand mining, bitumen upgrading, and oil combustion in the AOSR (Landis et al., 2012; Landis et al., 2017; Philips-Smith et al., 2017; Landis et al., 2019a; Landis et al., 2019b). These elements show a general spreading in spatial extent between 2008 (Appendix Fig. B.16a; Fig. 7a) and 2014 (Appendix Fig. B.16b; Fig. 7b) likely

reflecting both expansion of mining operations and the increase in the amount of bitumen upgraded between 2008 and 2014. Ni concentrations significantly increased primarily along a northwest – southeast transect through the AOSR. Ni increases in the central portion of the domain associated with surface oil sand production activities ranged from 23% (D4) to 35% (F5), but increased the most in the far western portion of the AOSR (B1, C1, D1) ranging from 42 to 52% (Appendix Fig. B.16e; Appendix Fig. B.18e). V concentrations significantly increased in (i) the central area of the modeling domain, where surface production activities increased between the two years (Fig. 7e; Appendix Fig. B.18f) resulting in zonal mean lichen concentration increases

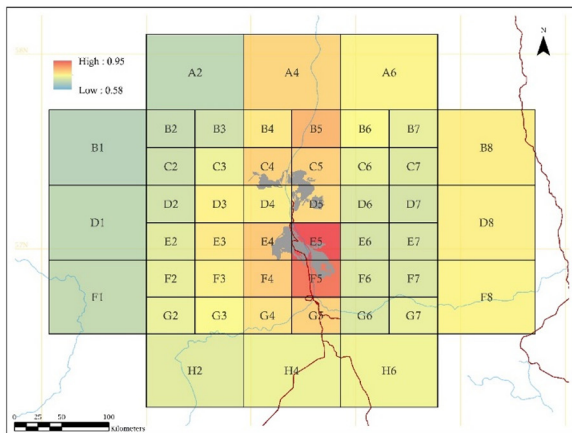
a. 2008 observed points and predicted surface



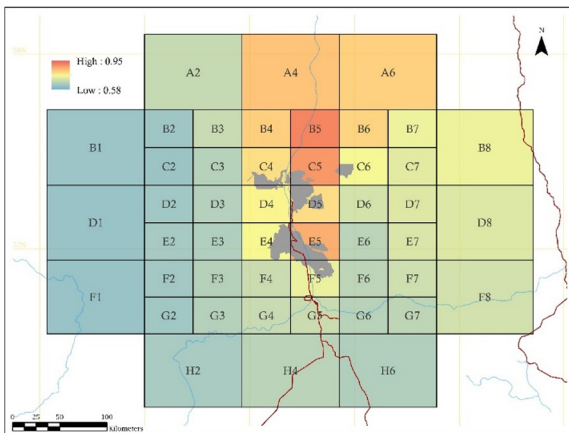
b. 2014 observed points and predicted surface



c. 2008 gridded zonal mean concentrations



d. 2014 gridded zonal mean concentrations



e. Δ_{TN} (2008 to 2014) gridded zonal mean concentrations with significant percent change

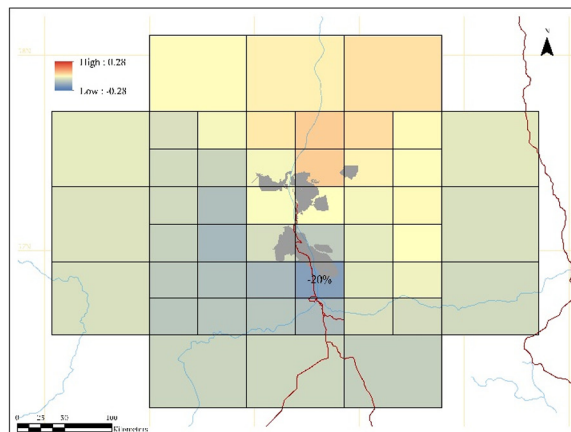


Fig. 5. Spatial and temporal analysis of total nitrogen (%) 2008–2014 using cokriging.

between 42 and 114%, and (ii) in the southeast portion of the domain in grids F7 and G7 resulting in zonal mean lichen concentration increases between 74 and 81%.

3.3.5. Calcium and strontium

Ca and Sr are primarily associated with limestone quarrying/crushing operations, mine haul roads, and general fugitive dust sources in the AOSR (Landis et al., 2012; Landis et al., 2017; Philips-Smith et al., 2017; Landis et al., 2019a; Landis et al., 2019b). Similar to Al and Fe, Ca interpolated surface maps (Fig. 8a–d) highlighted increased mine haul road construction and utilization activity, and the development/

utilization of unpaved parking and other surface activities in the southeast portion of the sampling domain along the highway corridor between Fort McMurray and Conklin. However, we were unable to detect the significance of the southern domain change in our gridded analysis. In contrast, Ca concentration in lichen significantly increased in grid cell C5 (Fig. 8e) possibly reflecting fugitive dust generation associated with the construction (2010–2012) and opening of the Imperial Oil Kearl surface mine in 2013. Sr was the only fugitive dust associated element with a significant decrease in lichen concentration between 2008 (Appendix Fig. B.17a) and 2014 (Appendix Fig. B.17b) in grids to both the east (F7, G7; 60–68%) and west (D3, E3, F4, G4; 43–51%) of

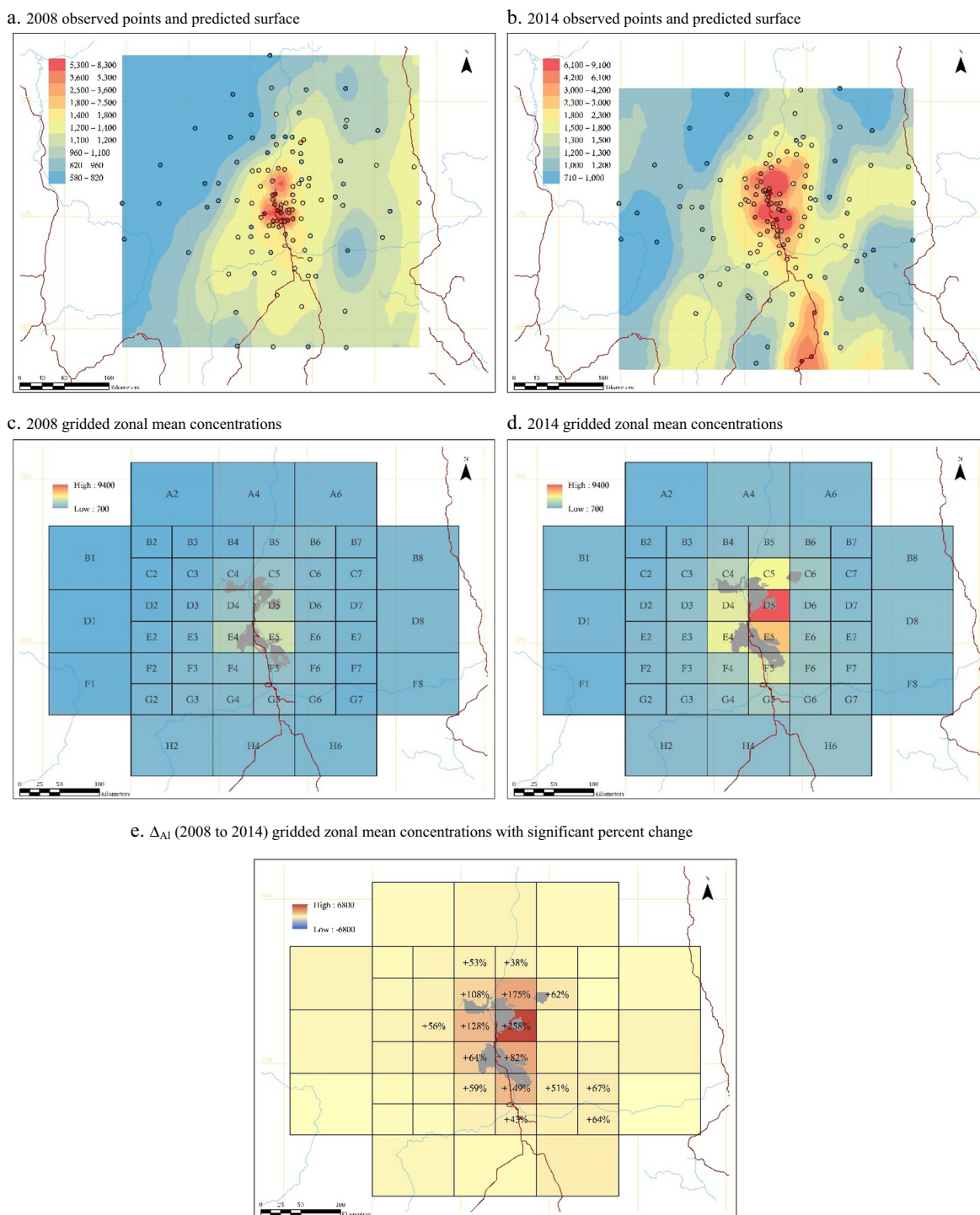


Fig. 6. Spatial and temporal analysis of aluminum ($\mu\text{g g}^{-1}$) 2008–2014 using cokriging.

the main oil sand production operations (Appendix Fig. B.17e; Appendix Fig. B.18h).

4. Conclusions

The atmospheric deposition patterns of TS, TN, Al, Ca, Fe, Ni, Sr, and V to the boreal forests surrounding the surface bitumen production and upgrading operations in the AOSR were investigated as part of a long-term in-situ lichen biomonitoring program. The epiphytic lichen species *H. physodes* was an effective indicator of atmospheric deposition that was sensitive to spatial and temporal changes in atmospheric

deposition from both gaseous and particulate emission sources in the region. Overall, results from this integrated analysis at both the site and gridded regional scales indicate that *H. physodes* lichen chemistry is an excellent tool to assess temporal and spatial changes in atmospheric deposition in the AOSR with respect to key emissions sources. Further, using lichens for biomonitoring is valuable in the AOSR and other remote regions where limited road access and electrical power distribution preclude traditional ambient monitoring.

H. physodes concentrations in the AOSR are comparable to other elevated sulfur deposition areas in the world (e.g., Finland, Norway, Switzerland) and in some cases published TS values are greater than

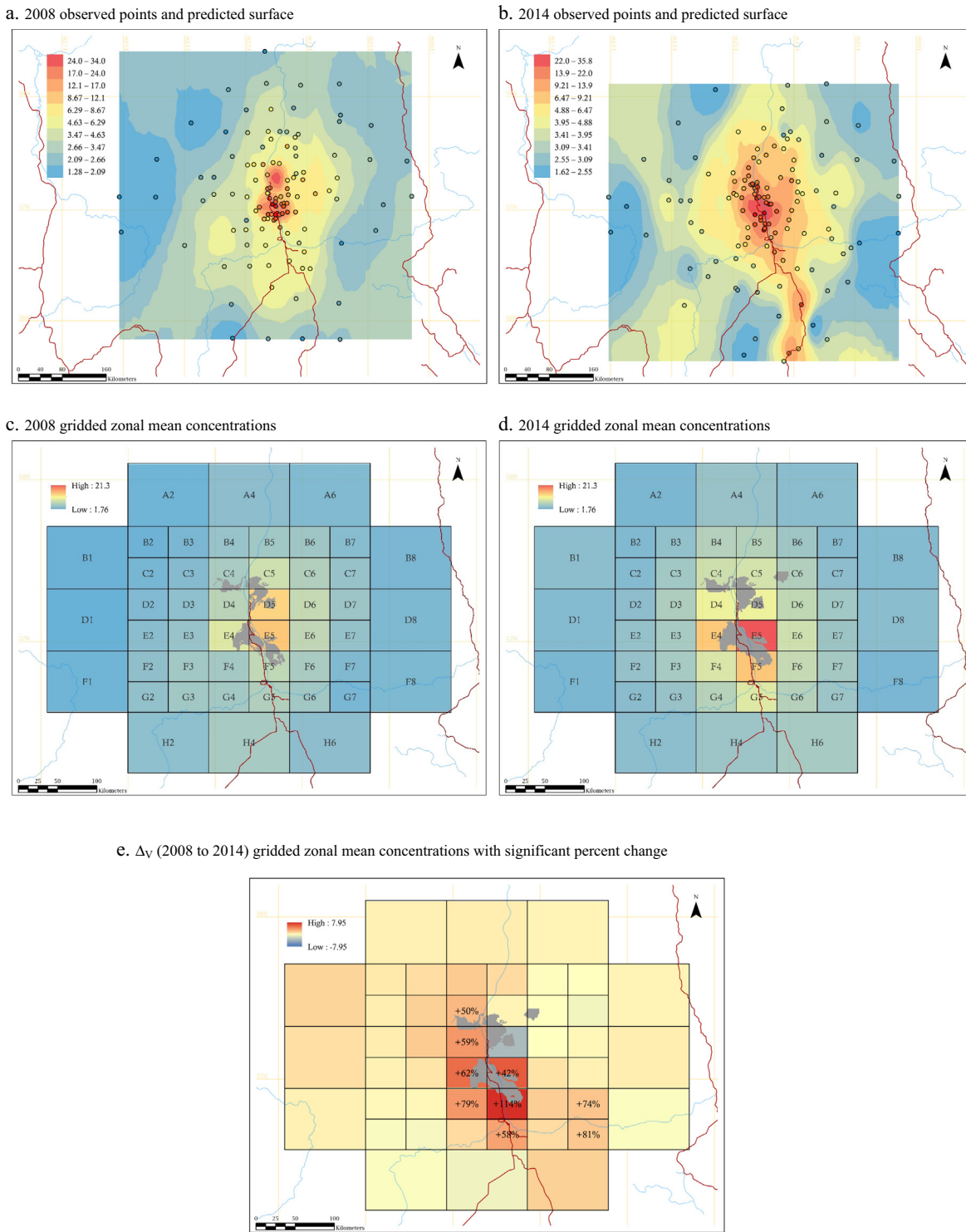
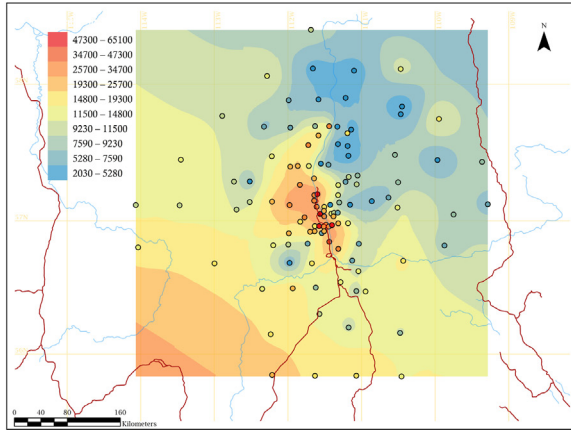


Fig. 7. Spatial and temporal analysis of vanadium ($\mu\text{g g}^{-1}$) 2008–2014 using cokriging.

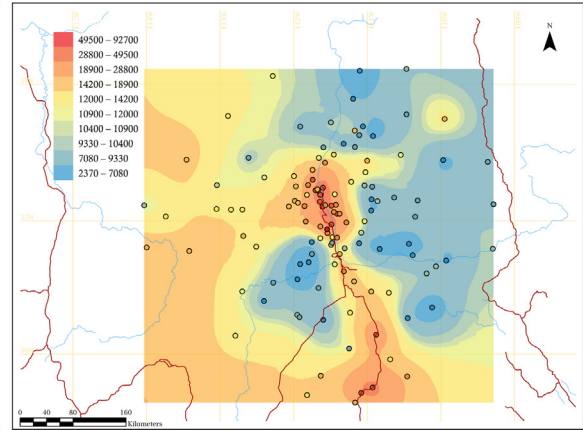
those measured in this study, suggesting that while the TN and TS levels are elevated in some portions of the AOSR domain, they have not reached an upper threshold of accumulation potential. Concentrations of Al, Fe, and Ca in some lichen samples from the AOSR are much greater than any published values, where the greatest Ca levels in *H. physodes* are almost a factor of three higher relative to the highest previously published value. It is unknown what the thresholds of accumulation of these elements are for *H. physodes*, and if these may be met at sites with heavy fugitive dust loading in the AOSR.

Site-specific time series analysis was conducted at eight FHM sites that were repeatedly sampled over the 2004 - 2017 study period. This analysis found the three sites near the surface oil sand mining and upgrading operations were associated with the highest overall element concentrations in *H. physodes*, the steepest gradients of increase, and the most significant trends. The concentrations of elements most associated with fugitive dust from surface oil sands production operations were most likely to have significantly increasing trends at proximal sites 1002 (Al, Ca, Fe, Sr, V), 1004 (Al, Ca, Fe, Sr, TS, V), and 1012 (Al, Ca, Fe,

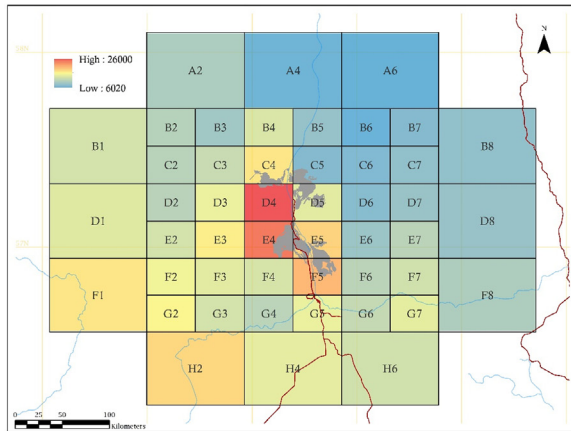
a. 2008 observed points and predicted surface



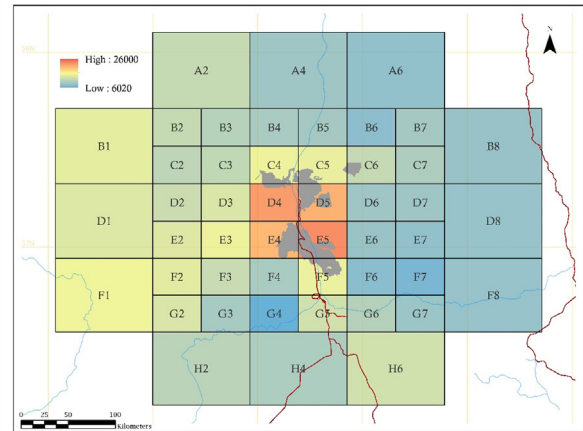
b. 2014 observed points and predicted surface



c. 2008 gridded zonal mean concentrations



d. 2014 gridded zonal mean concentrations



e. ΔC_a (2008 to 2014) gridded zonal mean concentrations with significant percent change

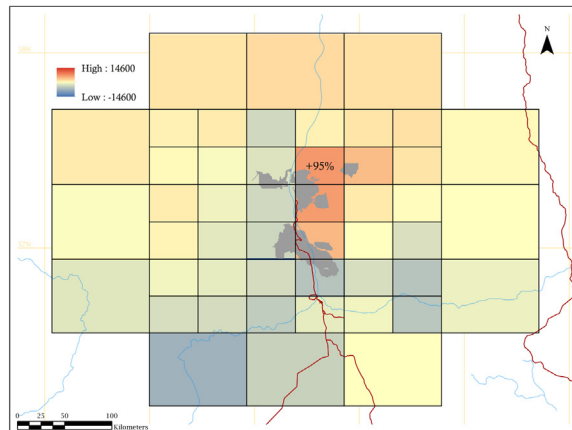


Fig. 8. Spatial and temporal analysis of calcium ($\mu\text{g g}^{-1}$) 2008–2014 using EBK.

Ni, Sr, V). Sites further away from the surface oil sand mining and upgrading operations (1001, 1006, 2001, 2010, 2013) were generally associated with the lowest concentrations, lowest rate of accumulation, and least number of significant trends. The enhancement ratios over the 2008–2014 sampling period ranged from 1.4 (TN) to 7.0 (Al) at the proximal sites 1004 and 2012, and from 0.9 (Ni) to 4.8 (Ni) at the distal sites 1001 and 2010, respectively.

Multiple regional scale geostatistical models were developed and evaluated to characterize broad-scale changes in atmospheric deposition from 2008 to 2014 based on changes in *H. physodes* elemental concentrations. EBK and cokriging lichen element concentrations with oil

sands mining, bitumen upgrading, petroleum coke materials handling, and limestone quarry/crushing production influence variables produced spatial interpolation estimates with the lowest validation errors. Gridded zonal mean lichen element concentrations were then calculated for the two comprehensive modeling years (2008, 2014) and evaluated for spatial and temporal change. Lichen TS concentrations significantly increased in every grid cell within the domain with the largest increases in the central valley in close proximity to the largest surface oil sand production operations, which is contrary to the regional SO_2 emissions inventory which indicates a reduction in emissions (Foster et al., 2019). The areal extent of fugitive dust element deposition

generally increased, but the greatest relative increases were observed in the outer grids of the enhanced deposition field reflecting new surface mining activity. Nitrogen deposition in the AOSR is increasing, as evidenced by the site-specific temporal analysis at 8 sites. However, this trend is obfuscated in the 2008–2014 spatial analysis by the relatively high 2008 lichen TN concentration values. Future lichen collection studies starting in 2021 will clarify this apparent discrepancy in the trend of TN atmospheric deposition between these two data analysis methodologies. Concentrations of TN in lichen are highly variable from site to site in areas of higher deposition and can be heavily influenced by wildfire events. *H. physodes* elemental concentrations can provide an integrated assessment of regional spatial and temporal deposition patterns by sampling large numbers of lichen biomonitoring sites, complementing the smaller number of active WBEA deposition and passive chemical substrate air monitoring sites in the AOSR.

Acknowledgements

This work was funded by the Wood Buffalo Environmental Association (WBEA), Fort McMurray, Canada (contracts T110-17 and T114-17) through the Oil Sands Monitoring Program (OSM). The content and opinions expressed by the authors do not necessarily reflect the views of the WBEA or of the WBEA membership. We thank Greg Brenner (Pacific Analytics Inc.) for contributing to the variance component analysis, the WBEA staff for their contributions in facilitating the collecting, cleaning, and analysis of lichen samples, and Martin Hansen (Rawin Consulting Corp.) for assisting with lichen data management. This paper is dedicated to the memory of Dr. Keith Puckett and Dr. Sagar Krupa.

Appendix A. Supplementary data

Supplementary data to this article can be found online at <https://doi.org/10.1016/j.scitotenv.2019.07.011>.

References

- Addison, P.A., 1984. Quantification of branch dwelling lichens for the detection of air-pollution impact. *Lichenologist* 16, 297–304.
- Addison, P.A., Puckett, K.J., 1980. Deposition of atmospheric pollutants as measured by lichen element content in the Athabasca oil sands area. *Canadian Journal of Botany-Revue Canadienne De Botanique* 58, 2323–2334.
- Alberta Energy Regulator, 2018. ST98: 2018: Alberta's energy reserves & supply/demand outlook. Government of Alberta March. https://www.aer.ca/documents/sts/ST98/ST98-2018_Executive_Summary.pdf, Accessed date: 16 February 2019.
- AMEC, 2000. Jack Pine Acid Deposition Monitoring Network Site Selection. Submitted to the Wood Buffalo Environmental Association by AMEC Earth and Environmental Ltd, Calgary (Report CE2078).
- Bates, D., Maechler, M., Bolker, B., Walker, S., 2015. Fitting linear mixed-effects models using lme4. *J. Stat. Softw.* 67 (1), 1–48.
- Berryman, S., Geiser, L.H., Brenner, G., 2004. Depositional gradients of atmospheric pollutants in the Athabasca Oil Sands Region, Alberta, Canada: an analysis of lichen tissue and lichen communities. Lichen Indicator Pilot Program 2002–2003. Report prepared for the Wood Buffalo Environmental Association, Fort McMurray, AB, Canada, p. 171.
- Berryman, S., Straker, J., Krupa, S., Davies, M., Ver Hoef, J., Brenner, G., 2010. Mapping the characteristics of air pollutant deposition patterns in the Athabasca Oil Sands Region using epiphytic lichens as bioindicators. Interim Report Submitted to the Terrestrial Environmental Effects Monitoring (TEEM) Science Sub-committee of the Wood Buffalo Environmental Association, Fort McMurray, AB, Canada.
- Brenner, G., 2005. Lichen data from the Athabasca Oil Sands Region, statistical report. Prepared for the Wood Buffalo Environmental Association, Fort McMurray, Alberta (June 2005. 93 pg).
- CE Jones and Associates, 2006. Terrestrial Environmental Effects Monitoring Acidification Monitoring Program: 2004 Sampling Event Report for Soils, Lichen, Understorey Vegetation and Forest Health and Productivity. Prepared for the Wood Buffalo Environmental Association, Fort McMurray, Alberta (October 2006. 858 pg).
- Clair, T.A., Percy, K.E., 2015. Assessing forest health in the Alberta Oil Sands Region. WBEA Technical Report 2015-03-01, 180pp and Appendices.
- Corbeil, R.R., Searle, S.R., 1976. Restricted maximum likelihood (REML) estimation of variance components in the mixed model. *Technometrics* 18, 31–38.
- Davies, M.J.E., 2012. Air quality modeling in the Athabasca Oil Sands Region. In: Percy, Kevin (Ed.), *Alberta Oil Sands: Energy, Industry and the Environment*. Elsevier, Oxford, England, pp. 267–309.
- Dobbs, D.L., 1985. Atmospheric emissions monitoring and vegetation effects in the Athabasca Oil Sands Region. *Ecological Research Monograph* 1985–5. Syncrude Canada Ltd (127pp).
- Douglas, G.W., Skorepa, A.C., 1976. Monitoring Air Quality with Lichen: A Feasibility Study 1976-2. Syncrude Canada Ltd. (69 pp).
- Edgerton, E.S., Fort, J.M., Baumann, K., Graney, J.R., Landis, M.S., Berryman, S., Krupa, S., 2012. Method for extraction and multi-element analysis of *Hypogymnia physodes* samples from the Athabasca Oil Sands Region. In: Percy, Kevin (Ed.), *Alberta Oil Sands: Energy, Industry and the Environment*. Elsevier, Oxford, England, pp. 315–342.
- Edgerton, E.S., Hsu, Y.-M., White, E.M., Landis, M.S., 2019. Ambient concentrations and total deposition of inorganic sulfur, inorganic nitrogen and base cations in the AOSR. *Sci. Total Environ.* (This Issue).
- Foster, K.R., Davidson, C., Spink, D., 2019. Introduction to the virtual special issue monitoring ecological responses to air quality and atmospheric deposition in the Athabasca Oil Sands region the wood Buffalo environmental Association's Forest health monitoring program. *Sci. Total Environ.* 686, 345–359.
- Garty, J., 2001. Biomonitoring atmospheric heavy metals with lichens: theory and application. *Critical Reviews in Plant Science* 20 (4), 309–371.
- Graney, J.R., Landis, M.S., Krupa, S., 2012. Coupling lead isotopes and element concentrations in epiphytic lichens to track sources of air emissions in the Athabasca Oil Sands Region. In: Percy, Kevin (Ed.), *Alberta Oil Sands: Energy, Industry and the Environment*. Elsevier, Oxford, England, pp. 343–372.
- Graney, J.R., Landis, M.S., Puckett, K.J., Studabaker, W., Edgerton, E.S., Legge, A., Percy, K.E., 2017. Differential accumulation of PAHs, elements, and Pb isotopes by five lichen species from the Athabasca Oil Sands Region in Alberta, Canada. *Chemosphere* 184, 700–710.
- Graney, J.R., Edgerton, E.S., Landis, M.S., 2019. Using Pb isotope ratios of particulate matter and epiphytic lichens from the Athabasca Oil Sands Region in Alberta, Canada to quantify local, regional, and global Pb source contributions. *Sci. Total Environ.* 654, 1293–1304.
- Hansen, B., 1989. Determination of nitrogen as elementary N, an alternative to Kjeldahl. *Acta Agric. Scand.* 39 (2), 113–118.
- Hartley, H.O., Rao, J.N.K., 1967. Maximum likelihood estimation for the mixed analysis of variance model. *Biometrika* 54, 93–108.
- Henderson, C.R., 1953. Estimation of variance and covariance components. *Biometrics* 9 (2), 226–252.
- Javari, M., 2017. Comparison of interpolation methods for modeling spatial variations of Precipitation in Iran. *International Journal of Environmental & Science Education* 12 (5), 1037–1054.
- Jennrich, R.I., Sampson, P.F., 1976. Newton-Raphson and related algorithms for maximum likelihood variance component estimation. *Technometrics* 18, 11–17.
- Jeran, Z., Jacimovic, R., Batic, F., Mavsar, R., 2002. Lichens as integrating air pollution monitors. *Environ. Pollut.* 120, 107–113.
- Kendall, M., 1938. A new measure of rank correlation. *Biometrika* 30, 81–89.
- Krige, D.G., 1951. A statistical approach to some basic mine evaluation problems on Witwatersrand. *Journal of Chemical Metallurgy of the Mining Society of South Africa* 52, 119–139.
- Krivoruchko, K., 2012. Empirical Bayesian kriging implemented in ArcGIS Geostatistical Analyst. *ESRI News* (Fall 2012 Issue), 6–10.
- Landis, M.S., Pancras, J.P., Graney, J.R., Stevens, R.K., Percy, K.E., Krupa, S., 2012. Receptor modeling of epiphytic lichens to elucidate the sources and spatial distribution of inorganic air pollution in the Athabasca Oil Sands Region. In: Percy, Kevin (Ed.), *Alberta Oil Sands: Energy, Industry and the Environment*. Elsevier, Oxford, England, pp. 427–467.
- Landis, M.S., Pancras, J.P., Graney, J.R., White, E.M., Edgerton, E.S., Legge, A., Percy, K.E., 2017. Source apportionment of ambient fine and coarse particulate matter at the Fort McKay community site, in the Athabasca Oil Sands Region, Alberta, Canada. *Sci. Total Environ.* 584–585, 105–117.
- Landis, M.S., Kamal, A.S., Edgerton, E.S., Wentworth, G., Sullivan, A.P., Dillner, A.M., 2018. The impact of the 2016 Fort McMurray Horse River Wildfire on ambient air pollution levels in the Athabasca Oil Sands Region, Alberta, Canada. *Sci. Total Environ.* 618, 1665–1676.
- Landis, M.S., Studebaker, W., Pancras, J.P., Graney, J.R., Puckett, K., White, E.M., Edgerton, E.S., 2019a. Source apportionment of an epiphytic lichen bioindicator to elucidate the sources and spatial distribution of polycyclic aromatic hydrocarbons in the Athabasca Oil Sands Region. *Sci. Total Environ.* 654, 1241–1257.
- Landis, M.S., Studebaker, W., Pancras, J.P., Graney, J.R., White, E.M., Edgerton, E.S., 2019b. Source apportionment of ambient fine and coarse particulate matter polycyclic aromatic hydrocarbons (PAHs) at the Bertha Ginter-Fort McKay community site in the Oil Sands Region of Alberta, Canada. *Sci. Total Environ.* 666, 540–558.
- Lantuejoul, C., 2002. *Geostatistical Simulation, Models and Algorithms*. Springer, Berlin, p. 256.
- Li, J., Heap, A.D., 2008. A Review of Spatial Interpolation Methods for Environmental Scientists. *Geoscience Australia*, p. 137 Record 2008/23.
- Nimis, P.L., Scheidegger, C., Wolseley, P.A. (Eds.), 2002. *Monitoring with lichens - monitoring lichens*. NATO Science Series IV. Earth and Environmental Sciences. vol. 7. Kluwer Academic Publishers, p. 408.
- Oxenham, D.J., Catchpoole, V.R., Dolby, G.R., 1983. A comparison of dry combustion and acid digestion for the determination of nitrogen in soil and plant material. *Commun. Soil Sci. Plant Anal.* 14 (2), 153–160.
- Pauls, R.W., Abboud, S.A., Turchenek, L.W., 1996. *Pollution Deposition Impacts on Lichens, Mosses, Wood and Soil*. Report prepared for Syncrude Canada Ltd., Fort McMurray, AB, p. 22.

- Percy, K.E., Krupa, S.V., 2012. Concluding remarks. In: Percy, Kevin (Ed.), *Alberta Oil Sands: Energy, Industry and the Environment*. Elsevier, Oxford, England, pp. 469–483.
- Pfeiffer, H.N., Barclay-Estrup, P., 1992. The use of a single lichen species, *Hypogymnia physodes*, as an indicator of air quality in northwestern Ontario. *Bryologist* 95 (1), 38–41.
- Phillips-Smith, C., Jeong, C.H., Healy, R.M., Zlotorzynska, E.D., Celio, V., Brook, J.R., Evans, G., 2017. Sources of particulate matter components in the Athabasca Oil Sands Region: investigation through a comparison of trace element measurement methodologies. *Atmos. Chem. Phys.* 17, 9435–9449.
- R Core Team, 2015. R Version 3.1.3 (2015-03-09). R: A Language and Environment for Statistical Computing. R Foundation for Statistical Computing, Vienna, Austria <http://www.R-project.org/>. Accessed date: 16 February 2019.
- Rhoades, F.M., 1999. A review of lichen and bryophyte elemental content literature with reference to Pacific northwest species. Prepared for the Department of Agriculture, Forest Service, Pacific Northwest Region (March 1999).
- Searle, S.R., 1987. *Linear Models for Unbalanced Data*. John Wiley & Sons, New York.
- Searle, S.R., 1994. An Overview of Variance Component Estimation. Biometrics Unit, Cornell University, Ithaca, N.Y (BU-1231-M).
- Searle, S.R., Casella, G., McCulloch, C.E., 1992. *Variance Components*. John Wiley and Sons, New York.
- Sheskin, D.J., 2000. *Handbook of Parametric and Nonparametric Statistical Procedures*, Second Edition. Chapman & Hall/CRC, Boca Raton, Florida.
- Speed, F.M., 1979. Choice of sums of squares for estimation of components of variance. Proceedings of the Statistical Computing Section. American Statistical Association, Alexandria, Va.
- Studabaker, W.B., Krupa, S., Jayanty, R.K.M., Raymer, J.H., 2012. Measurement of polynuclear aromatic hydrocarbons (PAHs) in epiphytic lichens for receptor modeling in the Alberta Oil Sands Region (AOSR): a pilot study. In: Percy, Kevin (Ed.), *Alberta Oil Sands: Energy, Industry and the Environment*. Elsevier, Oxford, England, pp. 391–425.
- Studabaker, W.B., Puckett, K.J., Percy, K.E., Landis, M.S., 2017. Determination of polycyclic aromatic hydrocarbons, dibenzothiophene, and alkylated homologs in the lichen *Hypogymnia physodes* by gas chromatography using single quadrupole mass spectrometry and time-of-flight mass spectrometry. *J. Chromatogr. A* 1492, 106–116.
- Sweeney, R.A., Rexroad, P.R., 1987. Comparison of LECO FP-228 “nitrogen determinator” with AOAC copper catalyst Kjeldahl method for crude protein. *Journal - Association of Official Analytical Chemists* 70 (6), 1028–1030.
- Tessier, A., Campbell, P.G.C., Bisson, M., 1979. Sequential extraction procedure for the speciation of particulate trace metals. *Anal. Chem.* 51, 844–850.
- Wetmore, C.M., 1987. Lichens and Air Quality in Boundary Waters Canoe Area of the Superior National Forest. Final Report. USDA Forest Service, Duluth, MN (18 p).
- White, J.R., Gubala, C.P., 1990. Sequentially extracted metals in Adirondack lake sediment cores. *J. Paleolimnol.* 3, 243–252.
- Wylie, E., 1978. Diversity and vitality of 10 epiphytic lichens measured over standardized sections of jack pine, white spruce and black spruce within an 11 kilometer radius from the Great Canadian Oil Sands Limited Complex in July 1977. Prepared for the Great Canadian Soil Sands Ltd by Loman and Associates (Calgary. 79pp).